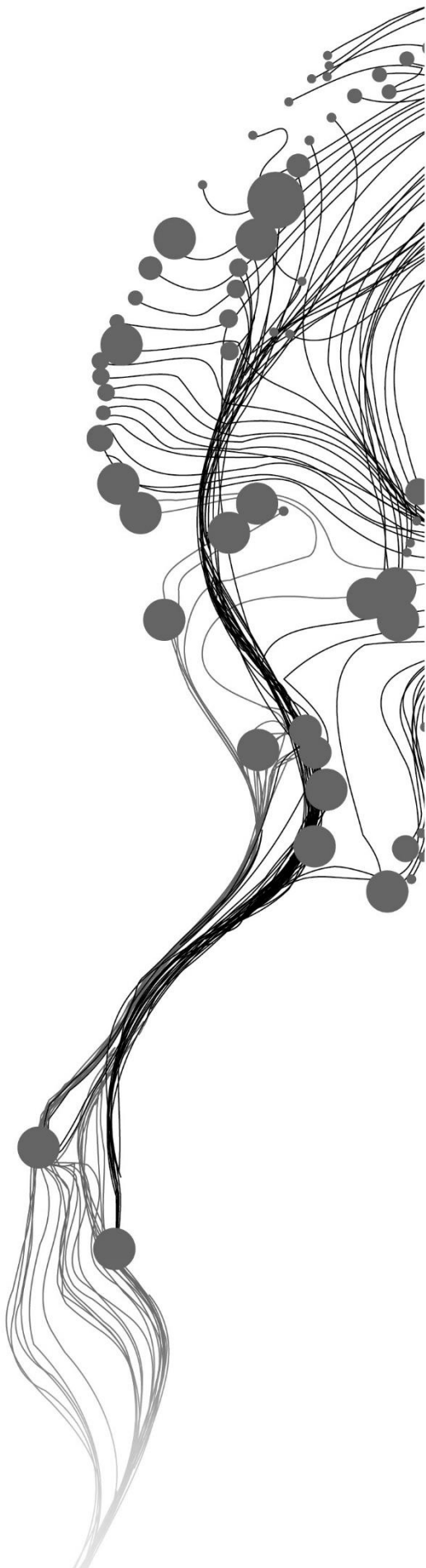


DETECTING OF NATURAL FOREST TO OIL PALM CONVERSIONS IN TROPICAL WETLANDS BASED ON SENTINEL IMAGERY USING DEEP

FAUZAN MUZAKKI
AUGUST, 2021

SUPERVISORS:
dr.I.C van Duren
dr R.V Mareto



DETECTING OF NATURAL FOREST TO OIL PALM CONVERSION IN TROPICAL WETLANDS BASED ON SENTINEL IMAGERY USING DEEP LEARNING

FAUZAN MUZAKKI

Enschede, The Netherlands, August, 2021

Thesis submitted to the Faculty of Geo-Information Science and Earth Observation of the University of Twente in partial fulfilment of the requirements for the degree of Master of Science in Spatial Engineering
Specialization: Spatial Engineering

SUPERVISORS:

dr. I.C van Duren

dr. R.V Maretto

THESIS ASSESSMENT BOARD:

dr.ir. T.A Groen (Chair)

dr. Leila Maria Garcia Fonesca (External Examiner, Instituto Nacional de Pesquisas Espaciais)

DISCLAIMER

This document describes work undertaken as part of a programme of study at the Faculty of Geo-Information Science and Earth Observation of the University of Twente. All views and opinions expressed therein remain the sole responsibility of the author and do not necessarily represent those of the Faculty.

ABSTRACT

Natural forest conversion to oil palm in tropical wetlands is dangerous for humans and biodiversity. Their capability to store carbon and flood prevention becomes the main reason that stakeholders should protect natural forest areas and tropical wetlands. The moratorium was enacted in 2018 to ban the expansion of oil palm plantations by companies or smallholder farmers through natural forest loss in tropical wetlands. Visual inspection of Google Earth imagery shows violations of the moratorium remains in Pelalawan Regency, Riau Province. The finding raises a question about the effectiveness of the moratorium to reduce oil palm expansion in tropical wetlands. Meanwhile, the Indonesian government legalized the conventional techniques (on-screen digitization) to map land cover in Indonesia. It is uncertain because prone to human error and time-consuming. Moreover, RPSO has been criticized by researchers because they have lack land trajectory information to track the data of previous land cover before becoming oil palm plantations. Remote sensing data has been used by academia to discriminate between land cover types and change detection. The synergies of Sentinel 1 and Sentinel 2 is the potential to overcome the limitation of Sentinel 1 and Sentinel 2 data alone for land cover classification and change detection. Moreover, the FCN model also has been used to automate semantic segmentation of remote sensing data in different resolutions and scales in the decoder-encoder style. This study examines which method (single imagery-based, synergy of Sentinel 1 and Sentinel 2 data) produces the reliable land cover classification. Then, using the best technique is to generate the map of natural forest to oil palm conversions in tropical wetlands, Pelalawan Regency, Riau Province, Indonesia. Also, this study wants to evaluate the moratorium's progress by comparing the change detection before (2016-2018) and after the moratorium period (2018-2020). This study figured out that the synergy of Sentinel 1 and Sentinel 2 data improved land cover classification compared to the single imagery-based technique. Using a GIS-practical approach, the post-classification composition technique achieved the highest accuracy over time with the averaged F1 score of 0.67. The natural forest to oil palm conversion map presents that the conversion patterns of the riparian zones and peatlands are different spatially. Conversions in riparian zones elongated follow the river, whereas conversions were irregularly distributed in peatlands. Regardless of misclassification in the conversion map, the moratorium looks like it did not work as it should be because this study observed the conversion area increased after the moratorium period, especially in riparian zones. Nevertheless, the method used in this study is more automated than conventional techniques used by the Indonesian government. Further investigation is necessary to improve the land cover classification and change detection accuracy using different sampling techniques and deep learning models. Moreover, the natural forest's trend, time, and magnitude to oil palm conversions based on Sentinel 1 and Sentinel 2 time-series data are also essential to further understand how effectively moratorium reduces oil palm expansion through natural forest loss.

ACKNOWLEDGEMENTS

I would like to express my deepest gratitude to my parents and brothers for their support until today. I would acknowledge the guidance of my supervisors, dr I.C van Duren and dr. R.V Maretto, for your patience, professional, scientific guidance, and funny discussion during the weekly supervisor meeting. I sincerely appreciate the advice that you gave to me. I enjoyed it.

Thanks to my friends in Spatial Engineering 2019-2021, especially for those of you who are patient with my pranks and antics in the study room and ITC International Hotel; Bisrat, Sarah, Ranju, David, Golnar, Chiara, Sander, and Kisanet.

I would express my appreciation to the Indonesian Student Association in the Netherlands and Enschede. They provided me with a place to grow and collaborate with people from different backgrounds and nations. Therefore, I can be a person who is not only beneficial to myself but also others.

Finally, I owe gratitude to the ITC Foundation Scholarship that allowed me to pursue a master's degree in ITC, University of Twente, The Netherlands. Thank you very much.

TABLE OF CONTENTS

1.	INTRODUCTION.....	1
1.1.	Oil palm trees in tropical wetlands, Indonesia	1
1.2.	The wicked problem of tropical wetlands protection	1
1.3.	Potential of Sentinel imagery for differentiating natural forest and oil palm trees and change detection...3	
1.4.	Deep learning in remote sensing applications	4
1.5.	Research Problem.....	5
1.6.	Research objectives and questions	6
2.	METHODOLOGY.....	7
2.1.	Study area.....	7
2.2.	Workflow	8
2.2.1.	Generating tropical wetlands layer	9
2.2.2.	Sentinel imagery	9
2.2.3.	Sentinel 1 data preprocessing.....	10
2.2.4.	Sentinel 2 data preprocessing	11
2.2.5.	Sampling.....	11
2.2.6.	Data preprocessing.....	12
2.2.7.	Land cover classification	13
2.2.8.	Hyperparameters tuning.....	14
2.2.9.	Accuracy assessment.....	15
2.2.10.	Change detection	16
2.2.11.	Rate of change analysis.....	16
3.	RESULT.....	17
3.1.	Selection of the optimum hyperparameters.....	17
3.2.	Qualitative comparison of land cover classification over methods.....	18
3.3.	The accuracy of land cover classification	21
3.4.	The natural forest to oil palm conversions	24
3.5.	The impact of the moratorium in reducing the natural forest loss through oil palm expansion	26
4.	DISCUSSION.....	28
4.1.	The importance of sampling design for land cover classification	28
4.2.	The quality of land cover classification	29
4.3.	The natural forest to oil palm change detection	30
4.4.	The implication of the moratorium in reducing oil palm expansion in the natural forest area.....	31
4.5.	Conclusion.....	31
4.6.	Recommendation	32

LIST OF FIGURES

Figure 1. Violation of aforementioned regulation in Pelalawan Regency, Indonesia, where the pink line covers the riparian buffer and the areas covered by the yellow polygon is oil palm. (Source: Google Earth image 2020)	2
Figure 2. A wicked problem framework.....	3
Figure 3. U-Net architecture (Olaf Ronneberger et.al, 2015).....	5
Figure 4. Study area	7
Figure 5. The workflow of the research	8
Figure 6. Tropical wetlands.....	9
Figure 7. Sentinel 1 preprocessing steps.....	10
Figure 8. Sentinel 2 preprocessing steps.....	11
Figure 9. Sampling patches distribution of Sentinel 2 data of 2016.....	12
Figure 10. Single imagery-based land cover classification scheme	13
Figure 11. U-net with early fusion architecture (R. V. Maretto, 2020)	13
Figure 12. Post-classification composition approach.....	14
Figure 13. Reference points distribution	16
Figure 14. The classified map of Sentinel 2 data with different set of hyperparameters.....	17
Figure 15. Loss curves produced by each set of hyperparameters (a) Set A, (b) Set B, (c) Set C, (d) Set D, (e) Set E.....	18
Figure 16. The comparison of each method to overcome missing lines on Sentinel 1 of 2018 images shown as a red circle (a) Sentinel 1 image of 2018, (b) Sentinel 1 classified map, (c) Early fusion classified map (d) Post-classification composition classified	19
Figure 17. The comparison of each method to overcome clouds on Sentinel 2 images observed in the red circle (a) Sentinel 2 image of 2020, (b) Sentinel 2 classified map, (c) Early fusion classified map, (d) Post classification composition classified map.....	20
Figure 18. The comparison for each of the methods continued to the discrepancy of land cover classes Sentinel 2 images (a) Sentinel 2 image of 2018, (b) Sentinel 1 classified map, (c) Early fusion classified map, (d) Post-classification composition classified map.....	21
Figure 19. The classified land cover maps of 2016, 2018, and 2020 are based on post-classification composition technique. The red circle shows misclassifications associated with artefacts observed.	24
Figure 20. The natural forest to oil palm conversions map.....	25
Figure 21. A subset of Planet imagery before the moratorium period (a) 2016, (b) 2018, (c) 2018 and conversion area classified. Blue circles observe real changes, whereas pink circles display unreal changes.	25
Figure 22. A subset of Planet imagery after the moratorium period (a) 2018, (b) 2020, (c) 2020 and conversion area classified. Blue circles observe real changes, whereas pink circles display unreal changes.	26

LIST OF TABLES

Table 1. Land cover classes and criteria.....	11
Table 2. Several sets of hyperparameters were tested in this study.....	14
Table 3. Results of hyperparameters tuning.....	17
Table 4. The confusion matrix of early fusion classified map of 2016.....	22
Table 5. The F1 score of a particular land cover class and averaged F1 score over methods.....	22
Table 6. The trend of natural forest areas.....	26
Table 7. The trend of oil palm areas.....	26
Table 8. The trend of the conversions.....	27

LIST OF ACRONYM

EF	: Early Fusion technique
ESA	: European Space Agency
FCN	: Fully Convolutional Network
GLCM	: Grey Level Co-Occurrence Matrix
S1	: Sentinel 1 data
S2	: Sentinel 2 data
MoEF	: Ministry of Environmental and Forestry, Indonesia
PCC	: Post-Classification Composition technique
QGIS	: Quantum Geographic Information System
SNAP	: Sentinel Application Platform
VH	: Vertical-Horizontal polarisation
VV	: Vertical-Vertical polarisation

1. INTRODUCTION

1.1. Oil palm trees in tropical wetlands, Indonesia

The tropical wetlands and natural forests are ecologically important and have climate benefits. They play an essential role to provide habitats for animals and livelihood for humans. Moreover, it stores numerous amounts of carbon as plant biomass in trees and peat soil. They also provide ecosystem services to local people, including providing timber and non-timber forest resources and maintaining the water level and quality. However, when farmers drain tropical wetlands and cut down the natural forest, it can support the growth of oil palm trees as one of the profitable crops in Indonesia (Gunawan, 2018).

Tropical wetlands are identical to peatlands and riparian zones in which both ecosystems are inundated by water permanently or seasonally (Kolka et al., 2016). When natural forests cover riparian zones, they act as an ecological corridor to wildlife along the river. Moreover, stream banks in riparian zones also protect humans from a flood. A few studies reported that when the natural forest along the river channel is converted to oil palm plantations by farmers, the geomorphic consequences increase runoff and shorten runoff time to river streams. It accelerates soil sedimentation on riverbeds (Horton et al., 2018). Consequently, riparian zones become flood-prone areas and endanger wild and human lives. Also, oil palm in riparian zones in Indonesia decreases water quality because herbicide, liming, and chemical fertilizer contaminate the river (Chellaiah & Yule, 2018). Then, if riparian zones are not protected, and actions against sustainability remain by stakeholders, aquatic ecosystems nearby riparian zones may be degraded, and biodiversity may go extinct in the future.

Oil palm trees are also extensively planted in peatlands. Peatlands in Indonesia is unique comparing to temperate peatlands in Europe. It is formed as an accumulation of forest trees, including branches, leaves, roots, and trunks, for over a thousand years to form deposits up to a thickness of 20 meters (Yustiawati et al., 2015). Temperate peatlands are mainly formed from mosses and shrubs. Nowadays, peatlands have been destroyed by farmers. They drain peatlands and clear natural forests to decrease the water level and provide space for new oil palm plantations. As a side effect of these activities, it accelerates the decomposition of organic matter, releasing carbon and methane into the atmosphere (Afriyanti et al. 2019). If land clearing remains in peatlands, numerous carbon and methane stored will be released into the atmosphere. As a consequence, peatlands may sink, causing floods, droughts, ruins of buildings or roads in the future.

1.2. The wicked problem of tropical wetlands protection

In recent days, the Indonesian government has been concern about the natural forest to oil palm conversion in tropical wetlands. They implemented some regulations to protect tropical wetlands and natural forests. In particular, President Instruction Number 18/2013 regulates the width of the riparian buffer zone for big (> 15 m width) and small (<15 m width) rivers that the government should protect from any conversions. In 2018, the government enacted the moratorium of oil palm that legally banned issuing new permits to clear the natural forest for new oil palm plantations, either by smallholder farmers or oil palm companies (Yusuf & Roos, 2017). However, farmers look like they violate the regulations since lack of law enforcement is also the central issue in Indonesia (Jong, 2021). By looking through Google Earth Map in 2020, it is proved that irregular oil palm trees were still found in riparian zones (Figure 1). It raises the question of

whether the regulations effectively reduce the natural forest loss through the oil palm expansion in tropical wetlands.



Figure 1. Violation of aforementioned regulation in Pelalawan Regency, Indonesia, where the pink line covers the riparian buffer and the areas covered by the yellow polygon is oil palm. (Source: Google Earth image 2020)

Oil palm trees in tropical wetlands have raised the alarm to pay attention to the moratorium's progress in reducing the natural forest loss through oil palm expansion in Indonesia. Jong (2021) reported that the government provided a platform in which people can check the progress of the moratorium. Nevertheless, they presented results based on Landsat 8 OLI and on-screen digitization as official data and technique (Ministry of Environmental and Forestry, 2017). Landsat 8 OLI images are less reliable due to cloud coverage and coarse spatial resolution (30 m). The conventional technique used is prone to human error and is time-consuming. Researchers should recommend an automated approach for land cover classification and change detection to the government, and thus they can tackle mentioned limitations.

The certification institution (e.g. Roundtable on Sustainable Palm Oil or RSPO) has been criticized because of the lack of information and knowledge about the land-clearing trajectory of oil palm growers (Gaveau et al., 2016). Although this criticism, they play a role to assess the Standard for Sustainable Palm Oil Production of oil palm companies and smallholder farmers globally. The standards ensure the growers apply sustainability practices. In addition, the certificate guarantees the oil palm-based products that customers consume are produced sustainably by the growers. As proof, the growers (e.g. oil palm companies or smallholder farmers) will receive the sustainability certificate. It allows their products to enter the European market because it is needed to fulfil mandatory requirements (Ruysschaert & Salles, 2014). One of the standards mentioned a prohibition from clearing any forests identified as having High Conservation Value or High Carbon Stock (RSPO, 2018). In fact, farmers likely confronted the standards (Figure 1) that oil palm trees remained in prohibited areas. Gaveau et al. (2016) commented that RSPO is also likely disputed by oil palm growers, claiming they plant oil palm trees in degraded and abandoned land. If the issue remains without any solutions, it will lead to further miss assessment and violations.

The effects of oil palm plantations converted from the natural forest in tropical wetlands become a primary issue in this study. A wicked problem framework is created to illustrate the problem complexity (Figure 2). It shows the consensus among stakeholders toward the certainty of knowledge on various aspects of the problem. Stakeholders know the regulations and Standard for Sustainable Palm Oil Production. However, the conflict between stakeholders becomes apparent when it comes to the importance of tropical wetlands. Each stakeholder (the government, oil palm companies, certificate institutions and local people) has different interests toward the natural forest and tropical wetlands, such as conservation, restoration, or oil

palm cultivation. The official method to support the moratorium's progress is considered less reliable. It contributes to the uncertainty of the information provided about the natural forest to the oil palm area conversion. Consequently, the debates on the topic become endless while tropical peatlands and the natural forest have been cleared.

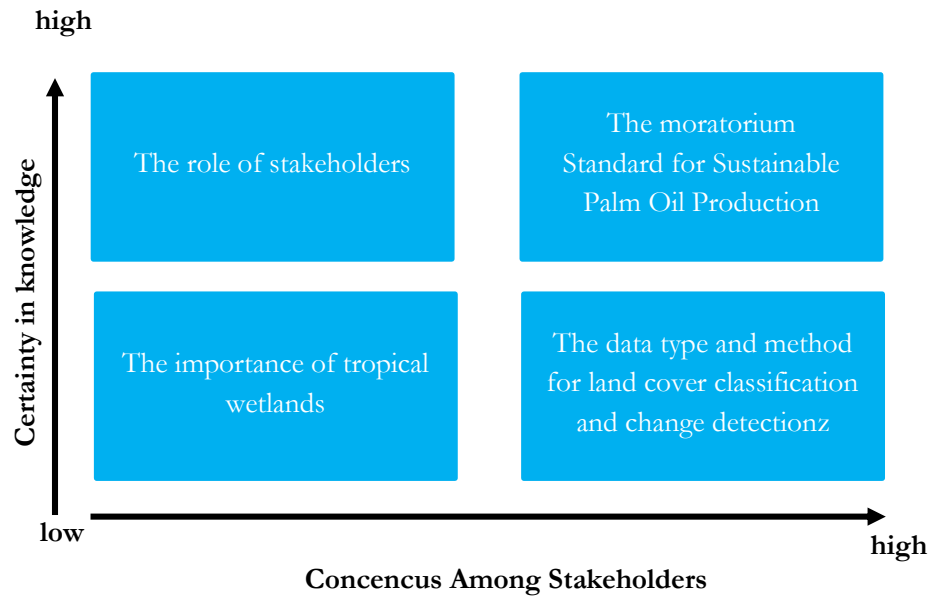


Figure 2. A wicked problem framework

1.3. Potential of Sentinel imagery for differentiating natural forest and oil palm trees and change detection

Since oil palm has become an attractive industrial crop, academia mainly uses remote sensing to provide methods and data to stakeholders. They support detecting illegal deforestation driven by oil palm and map land cover classes to demarcate oil palm and natural forest boundaries (Chong et al., 2017). Thanks to the European Space Agency (ESA) that launched Sentinel 2 (S2) in 2015, it has demonstrated an excellent potency for land cover mapping and change detection with 10-m resolution images. Descals et al. (2019) achieved an overall accuracy of 90% using Sentinel 2 data to separate smallholders and industrial oil palm areas in Riau Province. Sentinel 2 was equipped with red-edge bands (B5, B6, and B7) that were useful for all-scale forest disturbance mapping due to their sensitivity to the chlorophyll content presented by Xu et al. (2019). For change detection, Close et al. (2021) demonstrated the potential of Sentinel 2 data regarding land conversion/changes. But, clouds in tropical areas often become a problem when researchers use Sentinel 2 images alone (Reiche et al., 2015).

Researchers have extensively used Sentinel-1 Synthetic Aperture Radar images (S1) because their active sensor can overcome cloud coverage issues on satellite imagery. Adeli et al. (2020) described that the SAR sensor could interact with the object at the macroscopic level, which is related to physical properties of the earth surface, such as structure, surface roughness, and moisture content. Ballester-berman & Rastoll-gimenez (2021) also showed the utility of S1 data for oil palm and natural forest discrimination using VV-VH backscatter in the riverine area, Africa. However, land cover classification and change detection in wetlands is challenging due to radar's double bounce could generate false detection. Complex surfaces with large branches and high-water content in natural forests and wetlands often illuminate SAR signals (Adeli et

al., 2020). A previous study by Makinde & Oyelade (2020) observed that Sentinel 1 images caused falsely classified bare land and forest known as water bodies around riparian zones. The same misclassification may also be apparent in peatlands. Approaches to compensate for the limitation of using S1 images alone are needed to enhance their reliability.

To overcome Sentinel 1 and Sentinel 2 limitations, the synergy of Sentinel 1 and Sentinel 2 images could be a promising approach. Pohl & Van Genderen (1998) introduced the fusion technique to generate fused images. This technique synergizes information from different sensors, providing more features to be extracted using a particular algorithm. Chatziantoniou et al. (2017) proved that the fusion of Sentinel 1 and 2 data improve land cover classification accuracy in wetlands. Clerici et al. (2017) also inspected that natural forest areas are distinguished well when the synergy of sentinel 1 and 2 images are used. Another widely known technique is post-classification composition, which incorporates ancillary data before, during, or after the image classification. The ancillary data could be spatial or non-spatial information that may refine the image classification. Thakkar et al. (2017) composed land cover classification derived from Maximum Likelihood Classifier (MLC), Normalized Different Water Index (NDWI), and Geographical Information System (GIS)-based information based on visual interpretation to reduce misclassifications of natural forest. Nevertheless, previous studies mostly tested Sentinel imagery application for land cover classification, but it was less for change detection studies. It can be an opportunity to explore further and understand how reliable these techniques are for change detection.

1.4. Deep learning in remote sensing applications

Deep learning (DL) has been introduced as a set of neural network-based algorithms that automatically learn features available in remote sensing data. It could compensate for feature extraction by humans because it is lack complexity. In the case of deep learning, learnt features are capable of representing high-level characteristics of the data, being also learning optimized for each classification process. In neural networks, hidden layers are available between the input layer and output layer. Hidden layers allow the information provided by satellite data is extracted before producing outputs in the prediction stage. Each layer in hidden layers is responsible for learning a particular feature of the input image, then transform it to a more abstract level (X. X. Zhu et al., 2017). With this multilayer transformation architecture, the invariance and selectivity of the representation are improved. Nowadays, DL has been employed in almost all major sub-areas of remote sensing studies, such as land cover classification (Bermudez et al., 2018; Ienco et al., 2019; Lyu et al., 2016) and change detection (Sefrin et al., 2021). To further understand DL performance further, it is necessary to test deep learning and remote sensing data to different issues, including the natural forest and oil palm conversion in tropical wetlands, Indonesia.

The Fully Convolutional Networks (FCN) model have been developed for semantic segmentation, which assigns a class label to each pixel in an image. It considers the entire spatial context around each pixel in several scales to produce their labels with embedded spatial information (Zhuang et al. 2019; Yuan et al., 2021). Features extraction of the FCN model is structured based on stacked convolutional layers in an encoder-decoder style, allowing features extraction in different resolutions and scales (Flood et al., 2019). The encoder downscales the input image to a coarser level through the pooling operations (red arrow in Figure 3). In contrast, the decoder upscales back the input image to the original resolution and scales. U-net is FCN -based model that is widely used to generate land cover classified maps. As shown in Figure 3, the U-net is also built following the concept of encoder-decoder style. The U-net also contains the skip

connections (grey arrows in Figure 3) used to pass low-level features from encoder to decoder path. It allows the model to preserve object boundaries that often vanish during downscaling (Zhang et al., 2020).

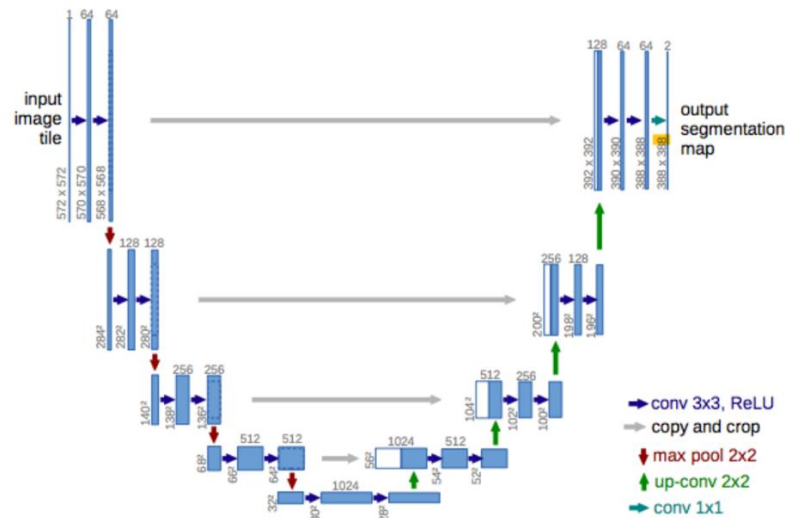


Figure 3. U-Net architecture (Olaf Ronneberger et.al, 2015)

A few researchers have used the U-net model for land cover classification and change detection. For example, Parente et al. (2019) combined U-net and Recurrent Neural Network (RNN) based on PlanetScope imagery that achieved 97% of overall accuracy. Maretto et al. (2020) achieved an overall accuracy of 95% with the spatiotemporal variation of the U-net architecture based on Landsat 8 Operational Land Imager (OLI). Nevertheless, limited studies combined the U-net and different techniques of Sentinel 1 and Sentinel 2 data synergy, such as fusion approach and post-classification composition for land cover classification and change detection using the FCN (U-net) model. It could be potential to extract more features and thus producing a high-accurate land cover classification and change map

1.5. Research Problem

The natural forest change driven by oil palm expansion in tropical wetlands causes biodiversity loss, carbon emission, and natural disasters. Even though the moratorium of oil palm was enacted in 2018 to protect tropical wetlands, there are indications of regulatory violations. The quality of the information provided by the government through satellite data is uncertain to human error due to the conventional technique and 30-m resolution satellite imagery used. It hampers the stakeholders to evaluate the progress of the moratorium further.

Land cover classification and change detection in tropical wetlands is challenging when Sentinel 1 (S1) and 2 (S2) products are used alone. Previous studies showed their peculiarities obscure in generating a high accurate mapping that may be potentially improved when the information from Sentinel 1 and Sentinel 2 are combined. Moreover, a Fully Convolutional Network (FCN) is also a promising model that could automatically learn feature information (e.g., edge, textures, and shapes) from the raw images provided by satellite data in a spatial context. Nevertheless, a few studies used synergetic information from multi-sensor images for land cover classification and change detection.

According to the opportunities mentioned above, this study wants to test which method between single images (S1 and S2 alone) and the synergy of Sentinel 1 and 2 data (fusion approach and post-classification composition) can produce the most reliable natural forest-to-oil palm change derived from land cover classifications using the FCN model. Furthermore, the land cover classification and change map produced in this work can help to evaluate the moratorium in reducing the natural forest loss through oil palm expansion in tropical wetlands.

1.6. Research objectives and questions

The main research objective is to compare the classification of single images (S1 or S2 data) and the synergy of Sentinel 1 and 2 data (fusion approach and post-classification composition) using the FCN model. The comparison is presented to test which method produces the most accurate land cover maps and the natural forest-to-oil palm change map in tropical wetlands. Next, the natural forest-to-oil palm change detection produced before is used to evaluate the moratorium of oil palm by comparing between before and after the moratorium period. The objective can be achieved through the following sub-objectives :

- a. To identify the accuracy of land cover mapping in tropical wetlands based on single images (S1 and S2) and the synergy of Sentinel 1 and 2 data using the FCN model
- b. To map the natural forest change into oil palm before (2016-2018) and after (2018-2020) the moratorium of oil palm in tropical wetlands.
- c. To evaluate the effect of the moratorium in reducing natural forest loss through oil palm expansion in tropical wetlands.

Research questions :

- a. To what extent do FCN and data types (S1, S2, and synergy of Sentinel 1 and 2 data) influence land cover classification accuracy in tropical wetlands?
- b. How was the natural forest area converted to oil palm before (2016-2018) and after (2018-2020) the moratorium in tropical wetlands?
- c. What is the moratorium's impact in reducing natural forest loss and oil palm expansion in tropical wetlands?

2. METHODOLOGY

2.1. Study area

Since reliable data is limited and restricted by stakeholders, the specific study area within Riau province was selected based on visual inspection of Planet imagery and online documents. The study area selection was considered to achieve the research objectives and answer research questions. It is necessary to identify areas based on specific criteria, whereby it could be assumed natural forests change into oil palm plantation has occurred in tropical wetlands. The criteria for selecting the study area are the following :

1. Peatlands and rivers are available in the study area to
2. Natural forest and oil palm areas are available in the study area.
3. Cloud-free Planet images of 2016, 2018, and 2020 are available to set reference points.

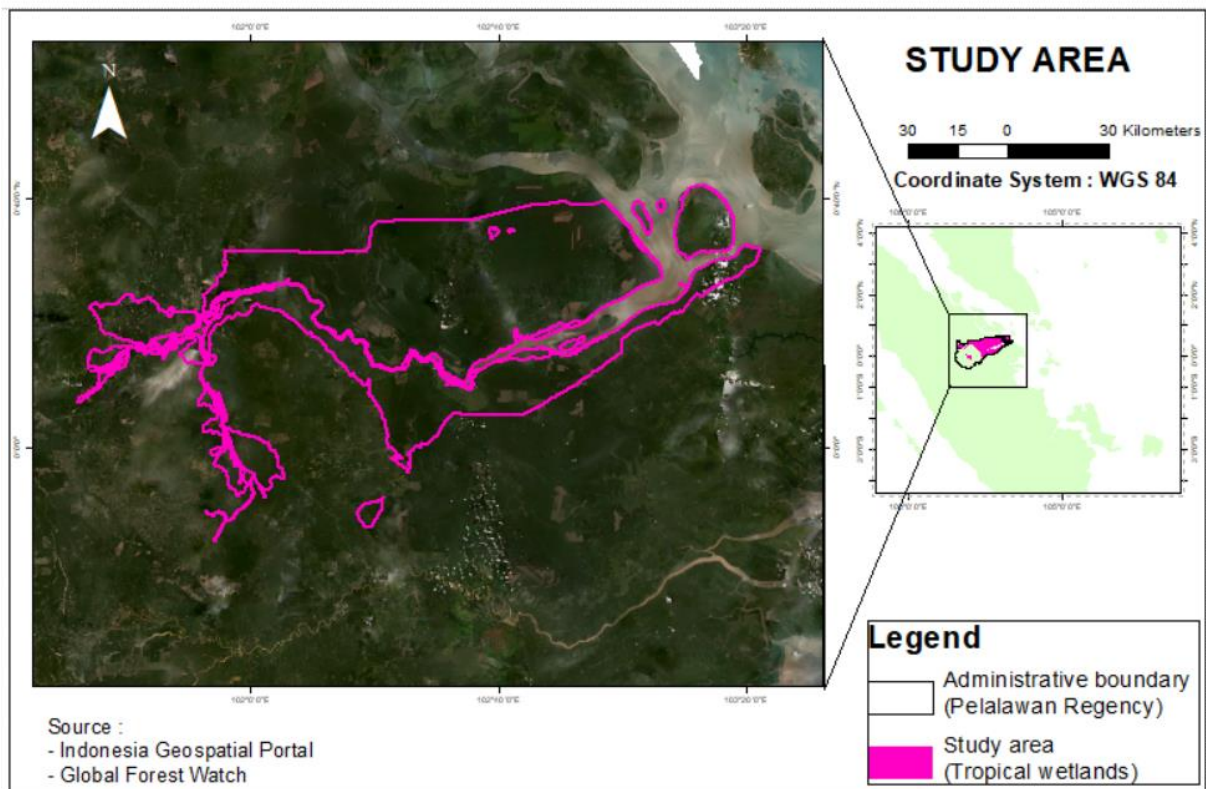


Figure 4. Study area

Based on those criteria, the tropical wetlands in Pelalawan Regency, Riau Province located on $00^{\circ}46'24''$ N - $00^{\circ}24'34''$ S and longitude $101^{\circ}30'37''$ E - $103^{\circ}21'36''$ E, was chosen as the study area in this study (Figure 4). This area covers peat swamps (east side), the Kampar river (large river), and small rivers. For this location, the number of cloud-free Planet images (<20%) in the study area are available and can be streamed online in QGIS through the Planet QGIS plugin (Planet, 2020).

2.2. Workflow

As shown in Figure 4, the workflow displays the steps to obtain results, answer the research questions and achieve the research objectives in this study.

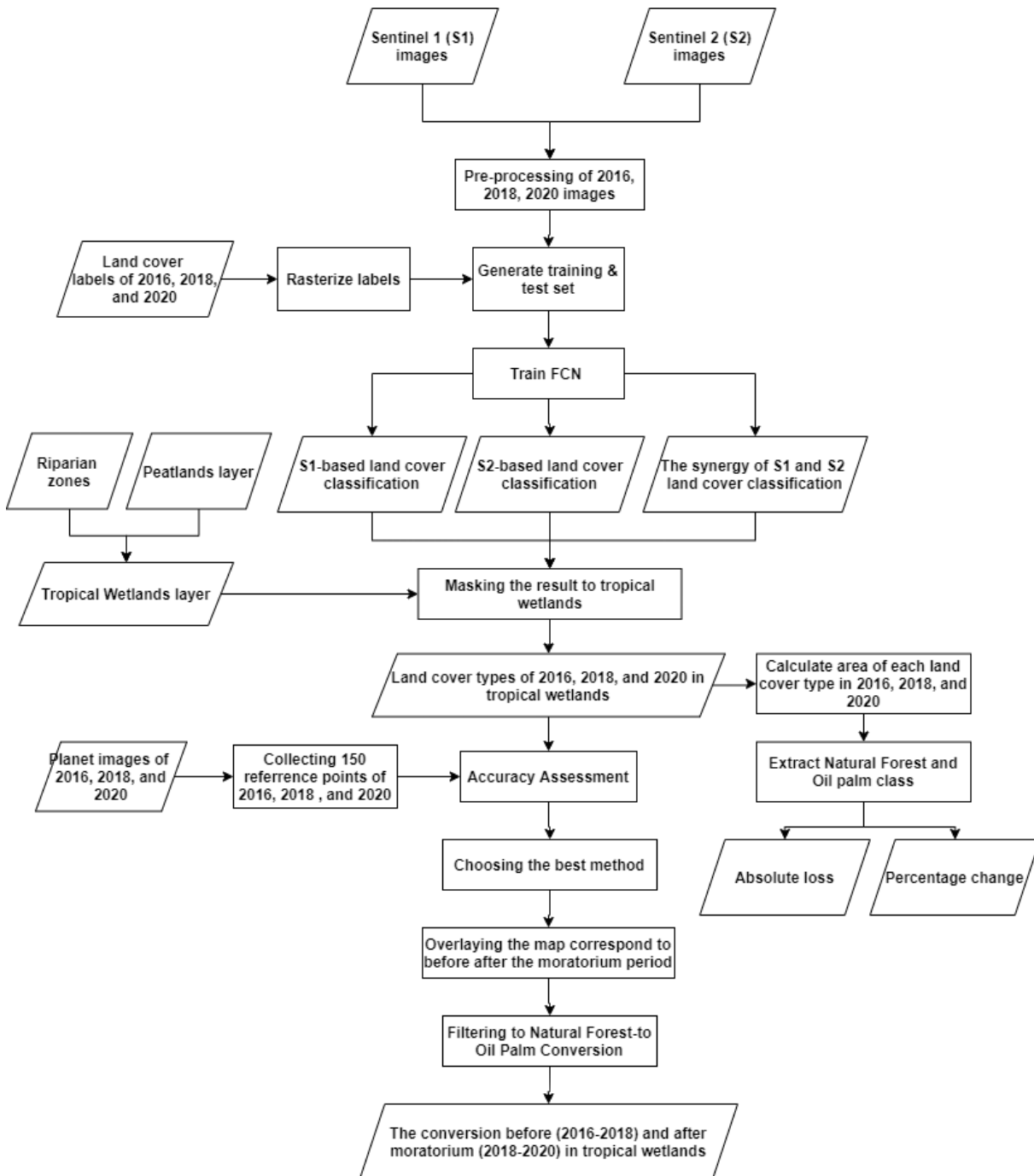


Figure 5. The workflow of the research

2.2.1. Generating tropical wetlands layer

The tropical wetlands layer in the Pelalawan regency was generated based on the available online dataset in the Indonesia Geoportal (<https://tanahair.indonesia.go.id/portal-web>) for the *river* layer (shapefile format) and the World Resources Institute (https://www.wri.org/resources/data_sets) for the *peatlands* layer (shapefile format). Also, the width of riparian buffer was applied to the *river* layer with regards to the Indonesia regulation, which is 50 m for small (<15 m) and 100 m for large rivers (>15 m). Then, both layers were merged to generate the *Tropical Wetlands* layer (shapefile format) (Figure 6).

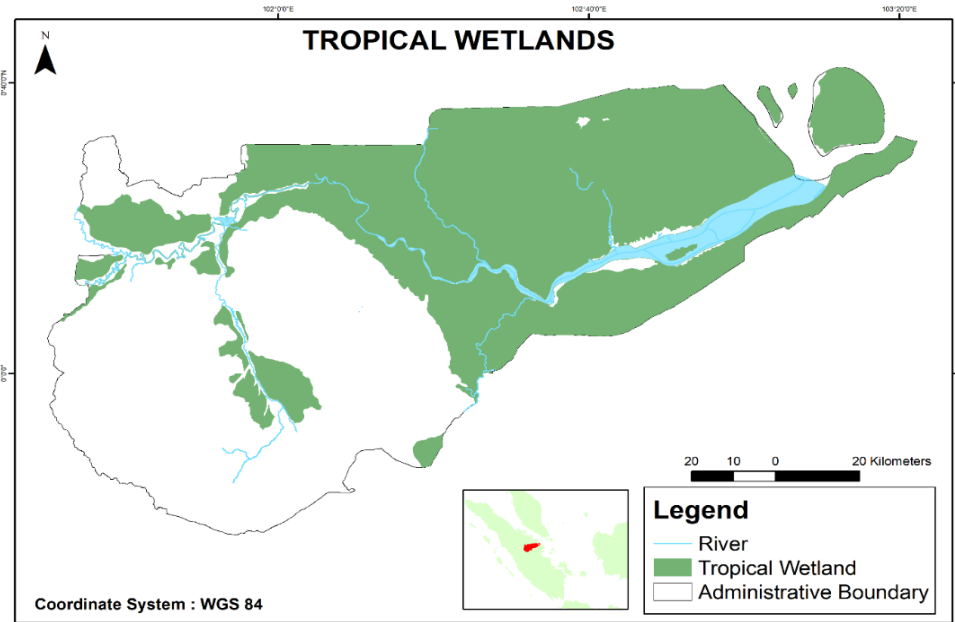


Figure 6. Tropical wetlands

2.2.2. Sentinel imagery

Sentinel 1 and Sentinel 2 images that are the Programme Satellite of the European Space Agency (ESA) were used in this study. They are online available and were downloaded from ESA Sentinel Scientific Hub (<https://scihub.copernicus.eu/>). Satellite images covering the study area consist of 5 tiles of Sentinel 1 images and 9 tiles of Sentinel 2 images (Appendix 1) before being mosaiced. The date of acquisition of each tile was taken in Indonesia's dry season (March-October) of 2016, 2018, and 2020 to avoid cloud covers on Sentinel 2 images and image desynchronization between Sentinel 1 and Sentinel 2 images, even between tiles of each satellite image.

To be specific, Sentinel 1 images are categorized as SAR (Synthetic Aperture Radar) data. It is a type of active data collection in which a sensor sends its own signals and receives the number of signals after interacting with the earth's surface. ESA's Sentinel 1 consists of Sentinel 1 A and Sentinel B, launched on April 2014 and April 2015. C-band is carried and can transmit in vertical (V) or horizontal (H), and then receive the signal in vertical (V) or horizontal (H). It is categorized into 4 possible polarizations: single-polarization (VV, VH) and dual-polarization (VV+VH, HH+HV). Moreover, the data is acquired in four modes: SM (StripMap), IW (Interferometric Wide Swath), EW (Extra-Wide Swath), and WV (Wave). On the ESA's website, two types of Sentinel 1 data are accessed: Ground Range Detected (GRD) and Single Look Complex (SLC). For this study, Sentinel 1 –GRD (S1) images with IW mode were selected. The S1 data were acquired images were selected in dual-polarization (VV+VH) to capture small and large land cover types on the earth's surface recommended by Steinhausen et al. (2018).

Sentinel 2 is an optical-passive satellite that relies on natural solar radiation reflected from the earth's surface. Sentinel 2 consists of Sentinel 2A and Sentinel 2B, launched in June 2015 and March 2017. It carries 13 bands at the spatial resolution of 10 m (four visible and near-infrared bands), 20 m (six red edge and shortwave infrared bands), and 60 m (three atmospheric bands) (Table 1). For this study, Sentinel 2 images with cloud coverage less than (20%) and Top-of Atmosphere (TOA) reflectances were used,

Table 1. List of bands on Sentinel 2 satellite

Band	Spectral region	Wavelength (μm)	Resolution (m)
Band 1	Coastal Aerosol	0.443	60
Band 2	Blue	0.490	10
Band 3	Green	0.560	10
Band 4	Red	0.665	10
Band 5	Vegetation Red Edge	0.705	20
Band 6	Vegetation Red Edge	0.740	20
Band 7	Vegetation Red Edge	0.783	20
Band 8	Near Infra Red (NIR)	0.842	10
Band 8A	Vegetation Red Edge	0.865	20
Band 9	NIR Narrow /Water vapour	0.945	60
Band 10	Short-Wave Infra-Red (SWIR)	1.375	60
Band 11	SWIR	1.610	20
Band 12	SWIR	2.190	20

2.2.3. Sentinel 1 data preprocessing

This stage is necessary to reduce radiometric bias, geometric distortion, and raw backscatter intensity. As a result, meaningful SAR data are acquired that represent actual radar backscatter of the object surface. To preprocess SAR images, the S1 preprocessing was preprocessed in open-source software known as the Sentinel Application Platform (SNAP), following preprocessing steps for land cover classification by Filipponi (2019) (Figure 7).

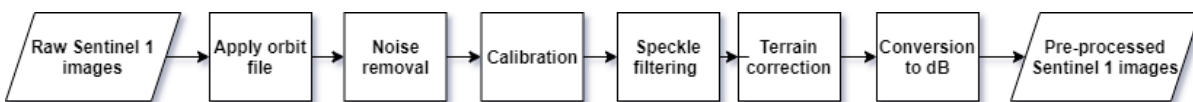


Figure 7. Sentinel 1 preprocessing steps

The explanation and logic for performing the preprocessing steps are described as follows :

- Apply orbit file;** SAR data are generally inaccurate. To tackle this, applying position correction in SNAP allows updating of satellite position for each SAR scene.
- Noise removal;** SAR data are disturbed by additive thermal noise and low-intensity noise on scene edges. These noises are caused by background energy and the change of Earth's curvature created during Sentinel 1 products generation.
- Calibration;** SAR data were converted to digital pixel values known as sigma nought (Σ_0). It is necessary to reduce radiometric bias remains and highlight radar backscatter of reflecting surface. Calibrated values represent a percentage of microwave energy received from the target surface, which depends on the characteristic of the target surface (e.g. shape, size, and moisture content), and the sensor system(e.g. polarization, and incident angle).

- d. **Speckle filtering;** SAR images has granular noises known as the *salt and pepper effect* because of the interference of waves reflected from all kinds of elementary scatter. Therefore, noises could be reduced, and thus the quality of images would be improved. In this step, the refined lee with a window size of 3x3 was applied to SAR scenes due to its ability to preserve edges and texture information on SAR data while reducing speckle.
- e. **Terrain correction;** SAR data frequently sense with different viewing angles, resulting in images distortion associated with the side-looking geometric. Digital Elevation Model (DEM) that automatically downloaded were used to compensate these distortions and reveal accurate geometric representations.
- f. **Conversion to dB;** SAR data were converted to physical quantity called the backscattering coefficient measured in decibel (dB) units. The dB value describes whether the radiated terrain scatters away from the SAR sensors or toward the SAR sensors.

2.2.4. Sentinel 2 data preprocessing

In this study, Sentinel 2 bands related to clouds were removed to reduce the atmospheric effect (Band 1, Band 2, Band 9 and Band 10), as Maretto et al. (2020) recommended. As similar to S1 preprocessing, S2 preprocessing steps were also executed in SNAP following steps in Figure 8.

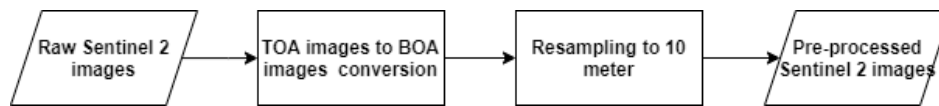


Figure 8. Sentinel 2 preprocessing steps

Firstly, S2 images of Top-of Atmosphere (TOA) reflectances acquired were converted to Bottom of Atmosphere (BOA) reflectances. It is necessary to reduce atmospheric, terrain, and cirrus distortion. To capture all-size natural forest change, Sentinel 2 –BOA images were resampled to 10 m resolution using bilinear interpolation technique, in which four pixels nearest *uncorrected* pixel are used to assign *corrected* pixel value. By applying this strategy, object edges/ boundaries would be preserved (Dahiya, Garg, & Jat, 2013).

2.2.5. Sampling

Samples referred to each land cover class were necessary to obtain the land cover classes' spectral signatures (Li et al., 2017). Due to it was not allowed to collect samples on the ground, high-resolution Planet was used. Samples were collected on small patches by generating a grid with a size of 300 by 300 pixels across the study area. The patch size was chosen larger than the top of targets to capture textures of each land cover class. After that, 110 patches were randomly chosen from the grid generated to collect samples. In order to train the model, corresponding labels accompanied each patch, in which labels represent land cover type on the ground. Labelling was identified by visual inspection and delineated by drawing polygons within patches collected. Labels naming followed land cover classes defined Ministry of Environment and Forestry (2017). It was aggregated into six categories (Table 1) to highlight necessary land cover classes (*natural forest and oil palm class*) from the other land cover types. This strategy was also implemented to obtain patches and labels of 2016, 2018, 2020 separately. Figure 9 shows an example of sampling patches distribution applied on Sentinel 2 images of 2016.

Table 1. Land cover classes and criteria

Aggregated category	Criteria	Data classes by MoEF
Natural Forest	Tree-covered areas	Primary dryland, secondary dryland, primary swamp, secondary swamp, and secondary mangrove forest

Aggregated category	Criteria	Data classes by MoEF
Oil Palm	Star-shaped structure area	Oil palm plantation
Bare land	Open areas without any land cover types	Bare land
Water	Land covered by an accumulation of water	River and lake
Other Land Covers	Anthropogenic landscape	Built-up area, agriculture area, acacia plantation, and road
Cloud (S2 images)	Cloud and cloud shadow	-

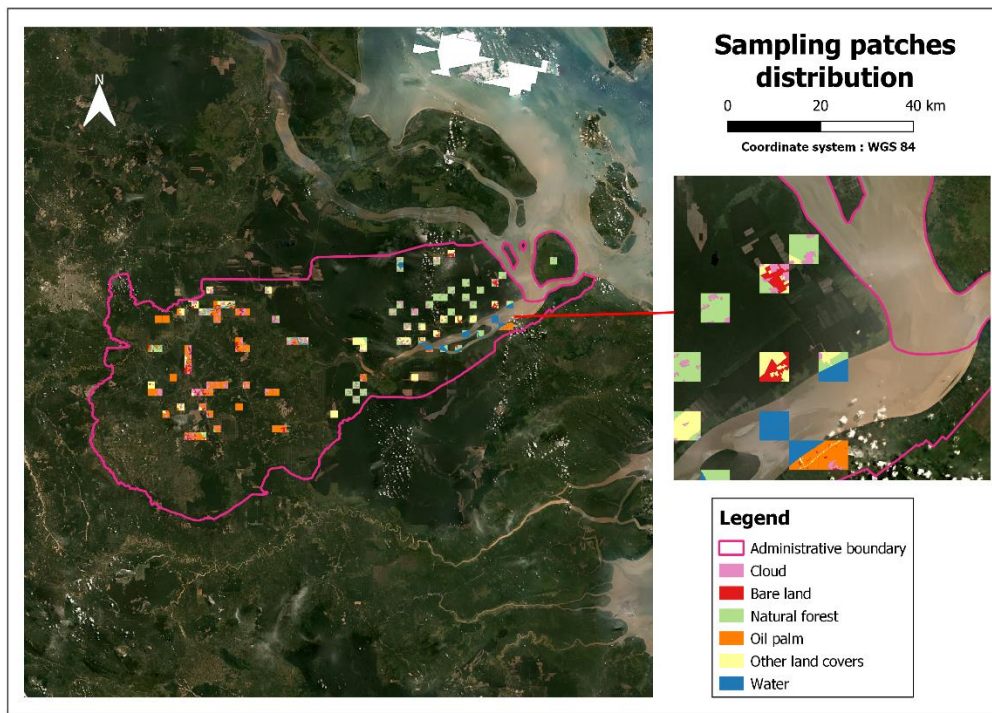


Figure 9. Sampling patches distribution of Sentinel 2 data of 2016

In addition, 110 patches were also used to slice the input image into image patches of 2016, 2018, and 2020. Patches with *no data* value were removed from the training data set. After slicing the input image, the whole set of paired image patches and labels of 2016, 2018, and 2020 were split into 80% for training (86 patches) and 20% for testing (24 patches). Training data is necessary to train the model, whereas testing data support model evaluation.

2.2.6. Data preprocessing

This stage refers to the technique of preparing training samples to make them suitable during training samples in the deep learning model. Ying (2019) noticed that overfitting is the common issue in supervised deep learning, which the model does not generalize well when the number of samples is too small or less representative. Due to overfitting, the model which may perform poorly on different datasets /predicted data.

To reduce overfitting, two strategies were applied: data augmentation and L2 regularization, as recommended by R. V. Maretto (2020). Data augmentation artificially inflates the size of the training set (Yan et al. 2019). It gives different transformations on the training set to make the model more invariant to the

target object's position in the image. Augmentations applied were rotations (90°, 180°, and 270°) and flips (left-right, up-down, and transpose) to the training set in this study.

This study used satellite imagery with the number of bands having numerous features to be learned by the model. Ying (2019) mentioned that overfitted models tend to consider all the features. However, not all features have a significant impact or are noise-free which are meaningless to the prediction. Thus, the effect of useless features needs to be limited. For this study, L2 regularization was applied. It includes less valuable features by giving them small weights instead of rejecting them to obtain as many features as possible (Ying, 2019).

Both strategies were performed on the fly during the training process. In addition, the same procedures were also applied over methods. Thus, the classified maps generated by several methods are comparable. The *DeepGeo toolbox* was used to perform mentioned strategies, generate a training and test set, train the deep learning model, apply deep learning classification based on a trained model, and analyze and visualize results (R. V. Mareto, 2019).

2.2.7. Land cover classification

In this study, three types of methods were tested for land cover classification: 1) Single imagery-based land cover classification, 2) Fusion-based land cover classification, and 3) Post classification composition. Mentioned methods were executed using the FCN model (U-net), developed by R. V. Mareto (2020). For single imagery-based land cover classification, the training set generated from Sentinel 1 and Sentinel 2 images each year trained the model to produce the classified map of each year (Figure 10).

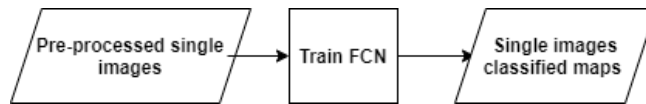


Figure 10. Single imagery-based land cover classification scheme

For image fusion, the early fusion approach was applied in this study. The early fusion scheme was inspired by R. V. Mareto (2020) (Figure 11). The early fusion approach was executed by concatenating the training set generated from S1 and S2 images of *N* timestamps before the training stage. As shown in Figure 11, *Image year 1* and *Image year 2* were replaced to Sentinel 1 and 2 images, respectively, to provide more information to the model and generate the classified map.

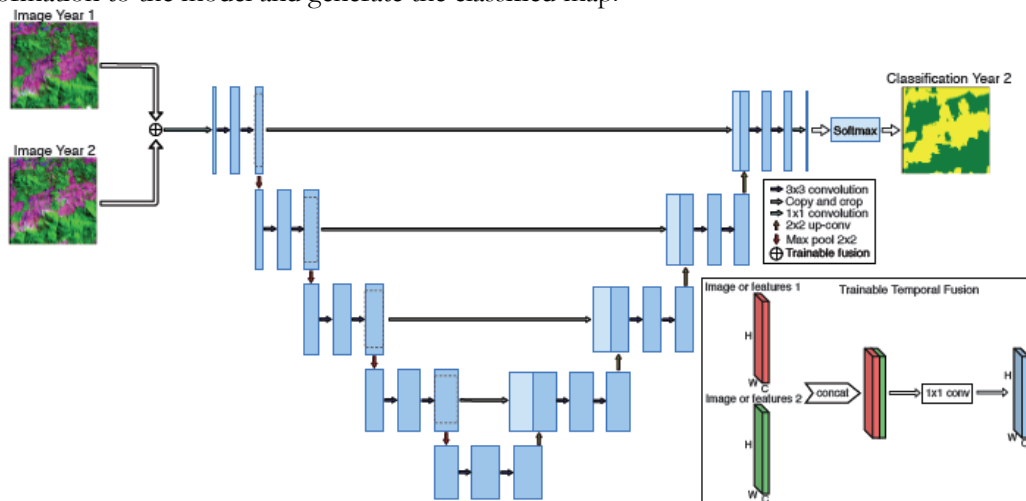


Figure 11. U-net with early fusion architecture (R. V. Mareto, 2020)

For post-classification composition, S1-based and S2-based land cover classifications of N timestamps were produced first. Then, pixels affected by cloud class in Sentinel 2 classified maps were masked and replaced with S1 classified maps to reveal land cover types under clouds over time (Figure 12). This technique was inspired by Thakkar et al. (2017).

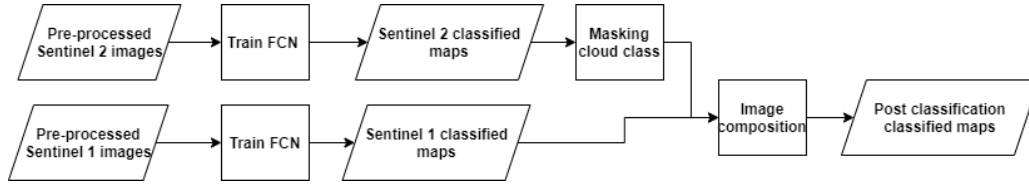


Figure 12. Post-classification composition approach

After land cover classification of each method over time were generated, the classified maps were masked corresponds to the *Tropical Wetlands* layer to focus on the study area

2.2.8. Hyperparameters tuning

The learning process of deep learning is controlled by hyperparameters (network parameters). Compared to parameters that the model learns, hyperparameters control the learning process of the model. For the model used in this work, they consist of the learning rate, the number of epochs, decay rate, and batch size. Learning rate controls how far the model updates the weights. The number of epochs describes the number of times that the learning algorithm passes through the entire training data during the backpropagation. One epoch compose of several steps of training, controlled by batch size. Batch size defines as the number of samples taken in each step. The decay rate allows the model to reduce the learning rate over time (You et al., 2019). In this study, exponential decay were used to prevent the model from stopping working in the middle of training process. This study tested several sets of hyperparameters, as shown in Table 2.

Table 2. Several sets of hyperparameters were tested in this study.

Set	Learning rate	Epochs	Decay rate	Batch size
A	0.1	100	0.95	5
B	0.1	200	0.95	5
C	0.01	100	0.95	5
D	0.01	200	0.95	5
E	0.001	200	0.95	5

Since the deep learning model is trained using a stochastic gradient descent algorithm, the loss function was set to calculate how well the model is trained for the given data. In this study, the loss function followed the *weighted cross-entropy (WCE)* to overcome the unbalanced number of samples over land cover types. The disparity number of samples was ignored by assigning the weight over land cover classes. This strategy allowed unbalanced data contribute to total loss during training (Phan & Yamamoto, 2020). It was performed before the training stage. Additionally, the loss curves were produced during training for monitoring the model performance. The calculation of WCE followed the equation described by Maretto et al. (2020):

$$WCE = -\sum_{c=1}^C Wc \sum_{i=1}^N Y_{true} \log(Y_{pred}) \quad (\text{Eq 1})$$

$$Wc = \frac{Ac}{Pc} \quad (\text{Eq 2})$$

Where Wc is a weight of each class defined as the average of all classes' proportions (Ac) divided by the proportion of N class (Pc), Y_{true} is the test data, and Y_{pred} is the prediction.

Due to lack of memory and overcome computation time, the Sentinel 2 image of 2016 was chosen for fine-tuning. For choosing optimum hyperparameters, the overall accuracy and loss curves were selected, followed by criteria: 1) the overall accuracy achieved the highest (Eq 3), and 2) the loss curves show a decreasing trend, as the model minimizes it. Mentioned criteria were necessary to ensure the model trained well with minimum loss/error.

$$OA = \frac{\text{the number of correctly classified pixels over land cover classes}}{\text{the number of reference data}} \quad (\text{Eq 3})$$

Once optimum hyperparameters were obtained, it attempted over methods in this study. To be more detail, the reference data is explained in the next step (accuracy assessment).

2.2.9. Accuracy assessment

Once methods generated results over time, the confusion matrix was also generated to assess the image classification accuracy. The accuracy of the FCN model on different methods was assessed by calculating three indices, specifically recall, precision, and F1 score (Eq 4-6). These indices can help to evaluate the accuracy and reliability of a particular class being mapped using several methods in this works. The recall is defined as a ratio of correctly classified pixels in the prediction map to the number of pixels in the reference points belonging to a certain class. Precision is defined as a ratio of the number of correctly classified pixels in the prediction map to the number of pixels classified into a certain class. F1 score is a harmonic mean of precision and recall (Graf et al., 2020).

$$R = \frac{TP}{TP+FN} \quad (\text{Eq 4})$$

$$P = \frac{TP}{TP+FP} \quad (\text{Eq 5})$$

$$F1 = 2 \frac{(P \times R)}{(P+R)} \quad (\text{Eq 6})$$

Where , P = precision ,R= recall , F1 = F1 score, TP = True Postive, FP = False Positive, FN = False Negative

In particular, recall (R) and precision (P) were computed based on True Positive (TP), False Positive (FP), and False Negative (FN) of each land cover type. TP means correctly classified pixels of a particular class in prediction and reference data. FP is the number of classified pixels that are not the same as reference data. FN denotes the number of pixels that are falsely detected by the classifier.

As this study mapped each land cover type over time, the averaged F1 score was also computed to determine which method produced the best results over time. It is computed by averaging the F1 score of a particular class over time. For reference data, 150 points of 2016, 2018, and 2020 were randomly distributed across the study area using random points generator in Quantum Geographic Information System (QGIS). Data attributes of reference points were collected using visual interpretation of high-resolution imagery (Planet

images). The reference points generated were also used to compute overall accuracy in hyperparameters tuning. Figure 13 shows the reference points distribution of 2016.

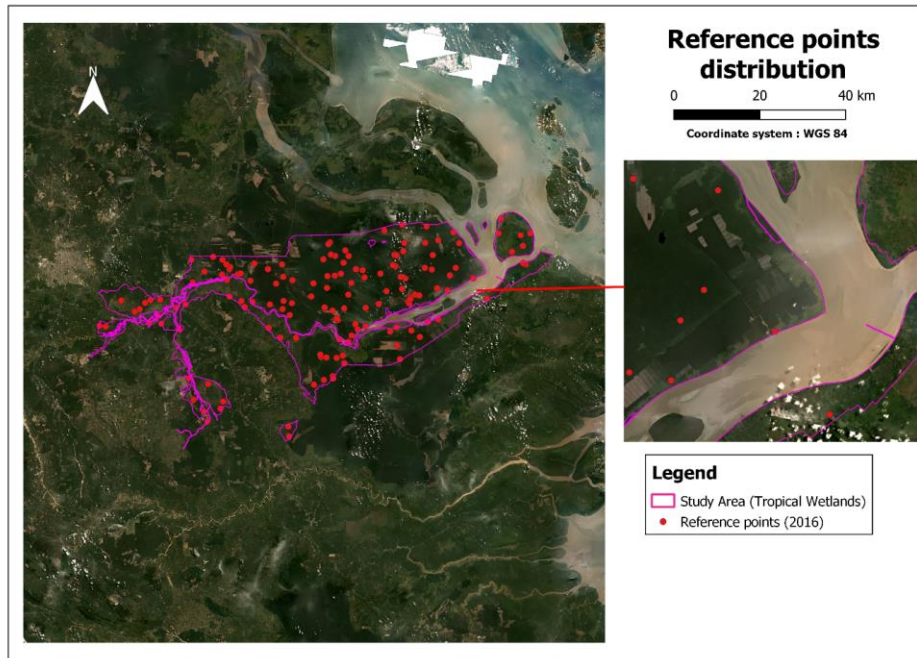


Figure 13. Sampling points distribution of 2016

2.2.10. Change detection

The goal of change detection is to obtain the change difference map between two or more images of the same area. Since this study is concerned with the natural forest to oil palm conversion, the post-classification technique was used to derive a change map. It worked by overlaying two input classified maps to produce "from-to" change information (Spruce et al. 2020). To accomplish that, the classified map of *year one* and *year two* were overlaid, correspond to 2016-2018 and 2018-2020. Next, the pixels associated with the natural forest class in *year one* and oil palm class in *year two* in the same area were extracted because this study wanted to present only the natural forest-to-oil palm change map.

2.2.11. Rate of change analysis

In this stage, the proportion of an area occupied by oil palm and natural forest throughout time were calculated. Then, the relative changes of both land cover classes were determined before (2016-2018) and after the moratorium period (2018-2020). It was followed by the determination of the relative change of changing area in both periods. For detailed analysis, the change analysis was measured in peatlands and riparian zones separately, following the mathematical formula by Suleiman et al. (2017) :

$$\Delta A = A1 - A2 \quad (\text{Eq 7})$$

$$PAC = \frac{\Delta A}{A1} \times 100 \quad (\text{Eq 8})$$

PAC= percentage area change (%)

ΔA = the difference of targeted area at the *period one* and *period two* (ha)

A1= targeted area at the beginning of the period (ha)

A2 = targeted area at the end of the period (ha)

3. RESULT

3.1. Selection of the optimum hyperparameters

After a thorough experiment, the overall accuracy (OA) and loss curves were produced to evaluate the training process. Table 3 displays the overall accuracy achieved using several sets of hyperparameters tested in this study. The result generated with each set is shown in Appendix 2. Implementing Set A and B did not improve the overall accuracy. It started to increase when Set C or the learning rate was reduced to 0.01. Yet, it stays the same using set D which used the learning rate of 0.01 and 200 epochs. The highest overall accuracy was reached when the learning rate of 0.001 and epochs of 200 was performed in Set E.

Table 3. Results of hyperparameters tuning

Set	A	B	C	D	E
OA	0.01	0.01	0.65	0.65	0.66

Figure 14 shows the results with each set applied. Set A and Set B show that the model could not predict well, as only *oil palm class* was mapped. The results of Set C, D and E display similar results. However, Set C and D have misclassification of *water class* and *natural forest class* (Appendix 2)

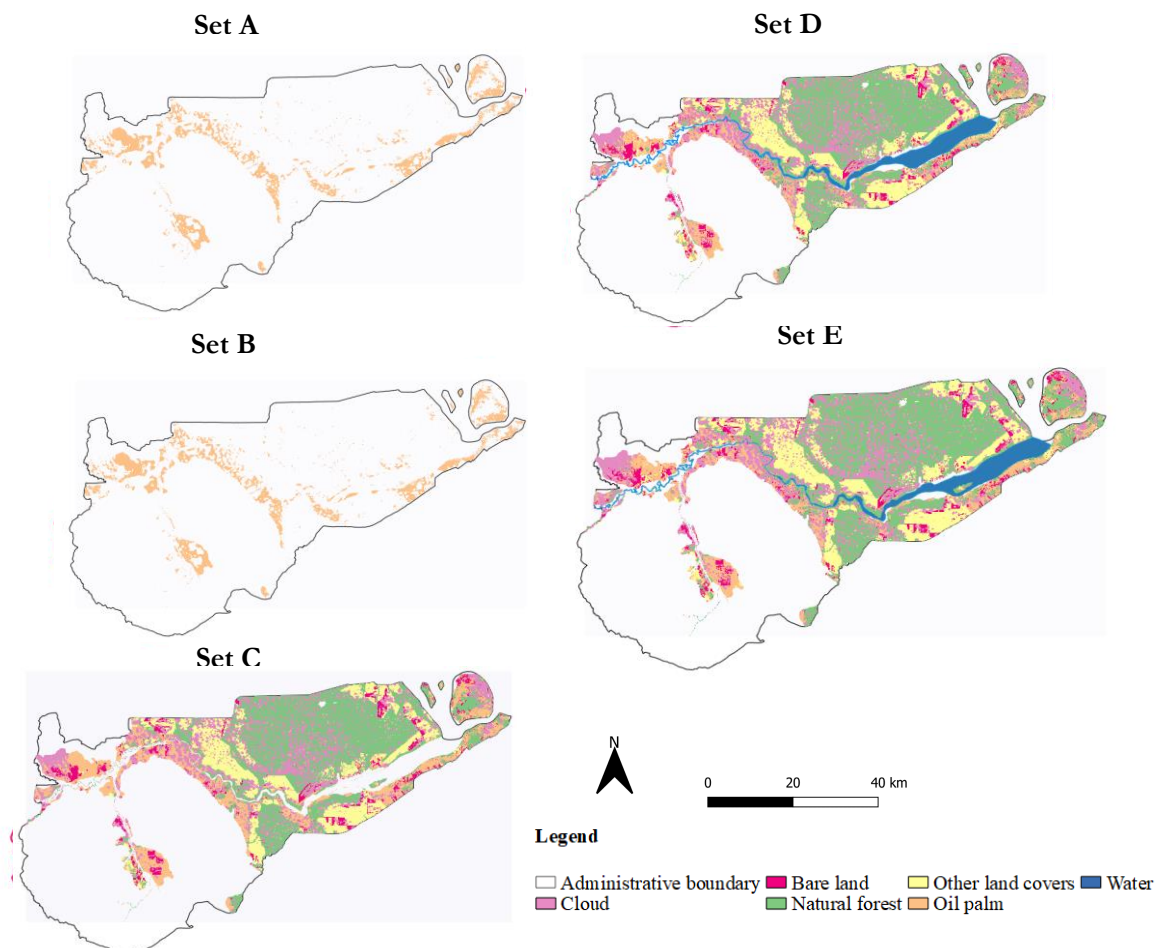


Figure 14. The classified map of Sentinel 2 data with different set of hyperparameter

To monitor the model performance, Figure 15 presents loss curves of each set of hyperparameters tested. This study aimed for a decreasing trend of the loss value, as the model learns the training data with minimum error. Loss curves exhibited a fluctuation trend when Set A and Set B were applied, meaning the model could not understand the training dataset. The loss started decaying when Set C was implemented. Still, the loss curves did not reach stability, indicating more epochs are needed. When Set D and E were applied, the loss decreased over time and got stability tren in the low loss value.

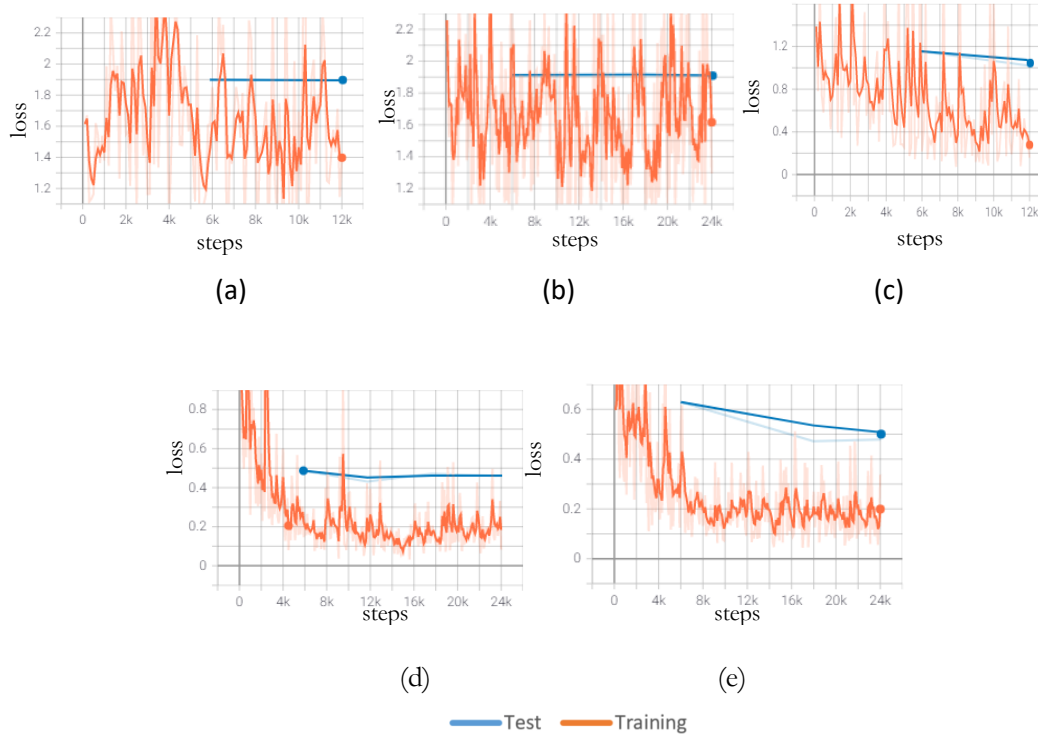
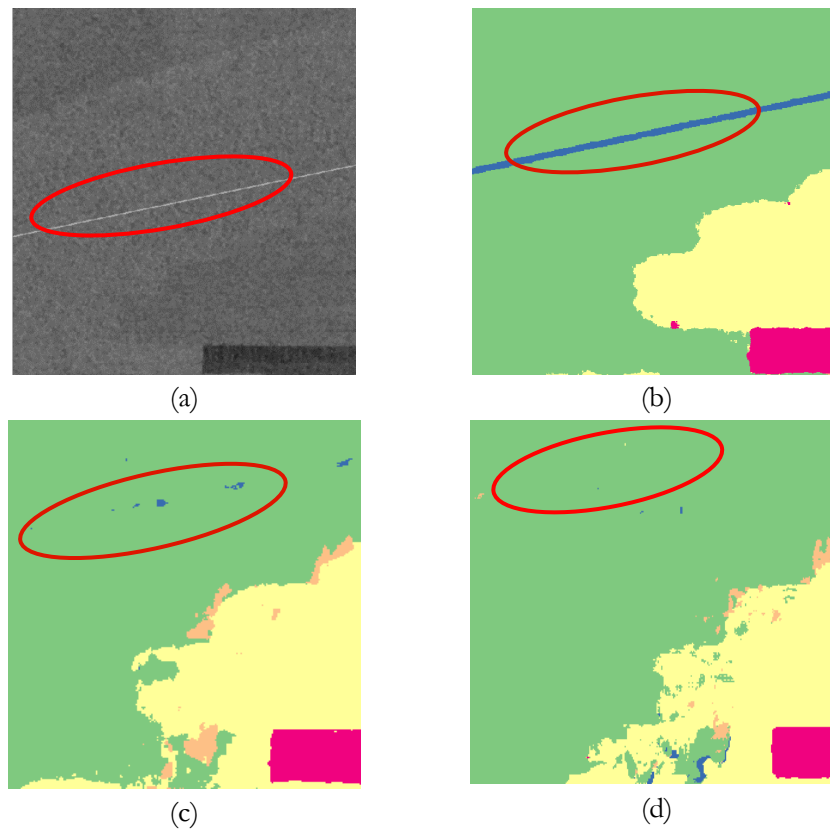


Figure 15. Loss curves produced by each set of hyperparameters (a) Set A, (b) Set B, (c) Set C, (d) Set D, (e) Set E.

According to Table 3 and Figure 15, this study figured out that decreasing the initial learning rate allows the model to reduce loss. On the other hand, increasing the number of epochs enable the model to reach minimum loss as more steps are available. The model achieved the highest overall accuracy when the loss curves have decreased over time. Once the best hyperparameters were achieved, it was implemented over methods (Appendix 3). Most of the overall accuracy achieved is more than 80% by the other techniques, except Sentinel 2-based technique due to clouds that obscure the validation of land cover types behind it.

3.2. Qualitative comparison of land cover classification over methods

This stage investigates the performance of different methods in removing artefacts, such as missing lines on Sentinel 1 images and clouds on Sentinel 2 images. It is necessary because the existence of artefacts hinder the estimation of oil palm and natural forest areas. As shown in Figure 16, missing lines were wrongly classified as *water class* in the Sentinel 1 classified map. Meanwhile, the post-classification composition approach successfully compensated missing lines in Sentinel 1 images. Meanwhile, small-size of missing lines were apparent in the early fusion classified map.



Legend

- Administrative boundary ■ Bare land ■ Other land covers ■ Water
- Cloud ■ Natural forest ■ Oil palm

Figure 16. The comparison of each method to overcome missing lines on Sentinel 1 of 2018 images shown as a red circle (a) Sentinel 1 image of 2018, (b) Sentinel 1 classified map, (c) Early fusion classified map (d) Post-classification composition classified

In Figure 17, the early fusion technique was not fully removed cloud covers on the Sentinel 2 scene of 2020. It looks like cloud shadow and thick clouds became a source of misclassifications. It wrongly classified as *oil palm, and other land cover class*. On the other hand, the post-classification composition approach performed superior in removing clouds on the Sentinel 2 image of 2020. The small pixels associated with cloud shadow and thick clouds were not fully removed. It was wrongly classified as *other land covers, oil palm, and water class*.

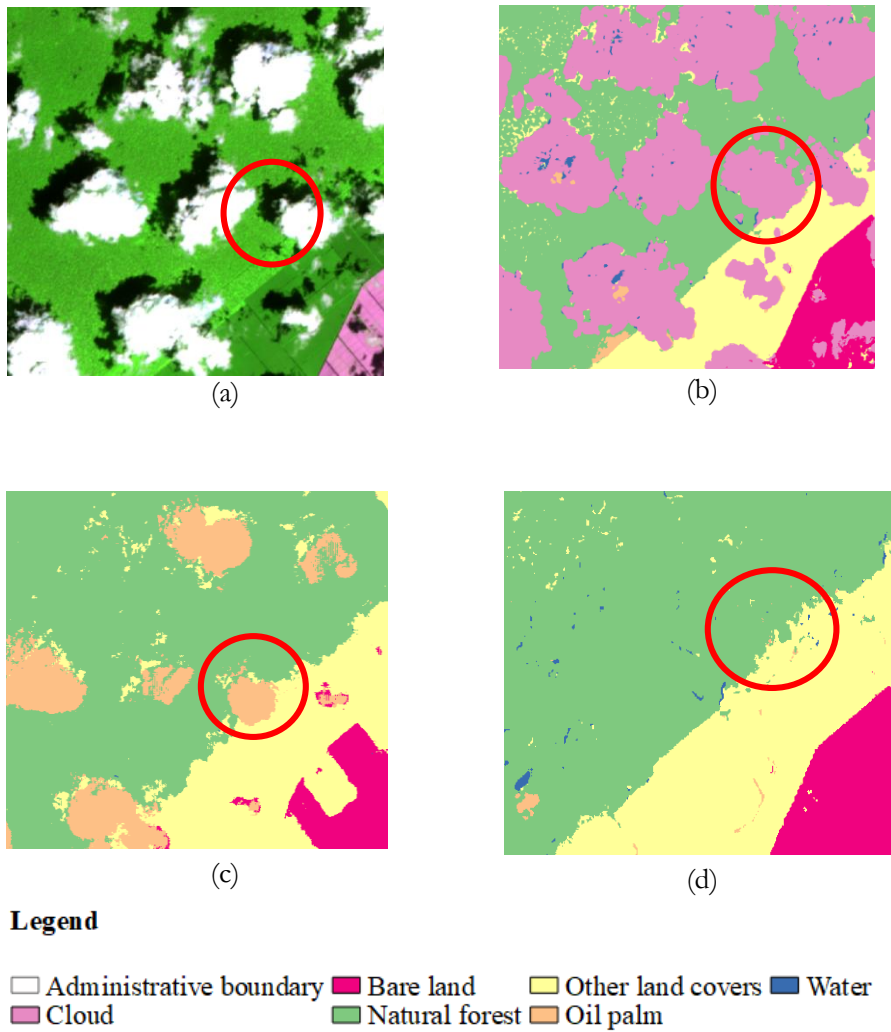


Figure 17. The comparison of each method to overcome clouds on Sentinel 2 images observed in the red circle (a) Sentinel 2 image of 2020, (b) Sentinel 2 classified map, (c) Early fusion classified map, (d) Post classification composition classified map.

Then, the comparison also investigates the capability of each method to distinguish land cover classes, especially between *natural forest* and *oil palm class*. In addition, Sentinel 2 classified maps are excluded in this stage because clouds were majorly mapped in the study area (Appendix 4). According to Figure 18, the synergy of Sentinel 1 and 2 data (Early Fusion and Post Classification Composition technique) improved the separability over land cover classes. Specifically, the border of natural forest and oil palm class shown by the early fusion and post-classification composition classified map are more prominent than Sentinel 1 data in Figure 18.

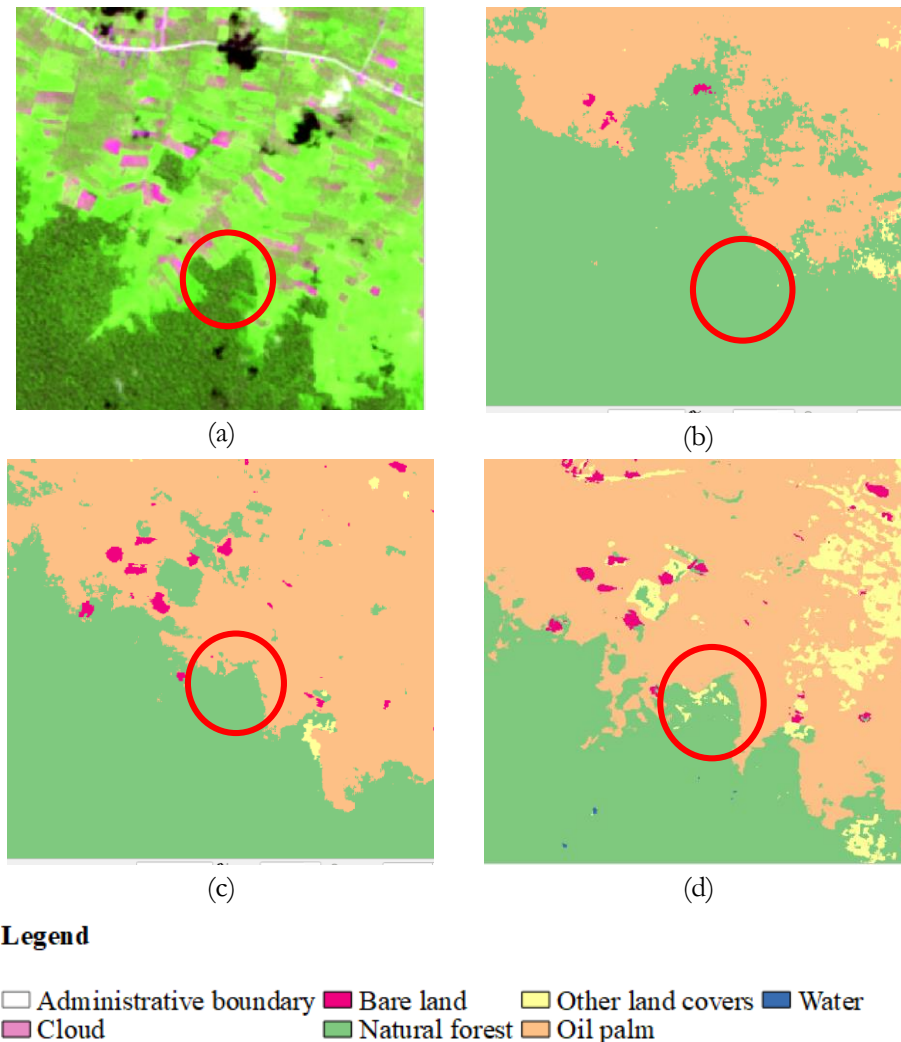


Figure 18. The comparison for each of the methods continued to the discrepancy of land cover classes Sentinel 2 images (a) Sentinel 2 image of 2018, (b) Sentinel 1 classified map, (c) Early fusion classified map, (d) Post-classification composition classified map.

3.3. The accuracy of land cover classification

Before deciding which method is the best, the confusion matrix of each method was generated (Appendix 4) to describe the performance of each method toward reference points collected. Table 4 shows an example of the confusion matrix of early fusion of 2016. The result revealed that the *oil palm class* in the reference points were wrongly classified as *bare land class* and vice versa, shown as 4 and 1 reference points (red in Table 4) were misclassified. Furthermore, *natural forest class* in the reference were mapped by the model as *oil palm*, and *other land covers class* (green in Table 4).

Table 4. The confusion matrix of early fusion classified map of 2016

Predicted	Reference						
	Land cover class	bare land	natural forest	other land covers	oil palm	water	Total
bare land	4	0	3	4	1	12	
natural forest	0	69	0	0	1	70	
other land covers	3	5	29	5	0	42	
oil palm	1	2	2	17	0	22	
water	0	0	0	1	3	4	
Total	8	76	34	27	5	150	

This study is interested in the quality of each method in delineating a particular class. Table 5 shows the F1 score of a specific land cover class over time and averaged F1 score over methods.

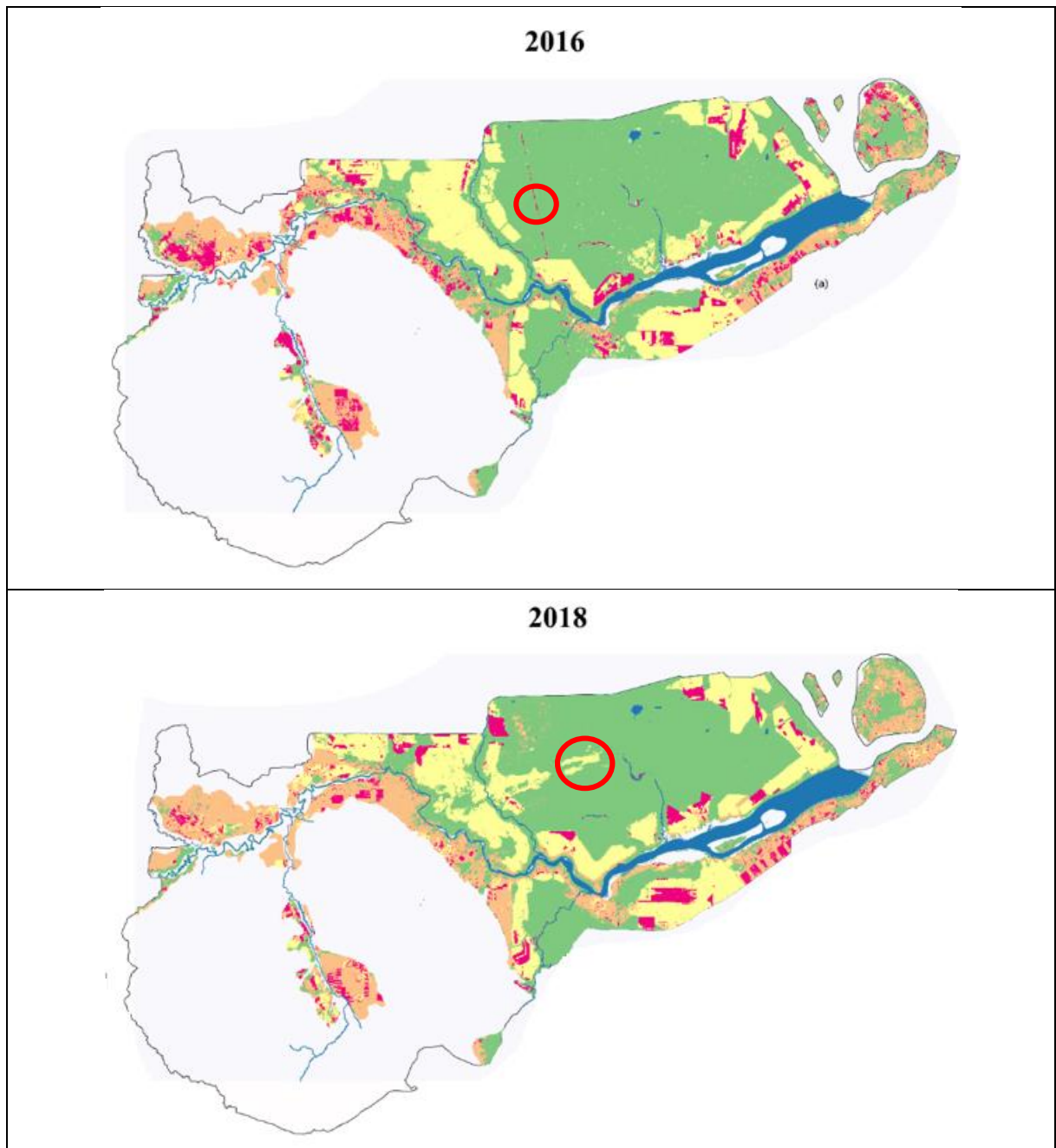
Table 5. The F1 score of a particular land cover class and averaged F1 score over methods

Dataset	Year	F1 score					Averaged F1 Score
		Bare land	Other land covers	Water	Natural Forest	Oil Palm	
Sentinel 1	2016	0.40	0.79	0.75	0.90	0.70	0.63
	2018	0.33	0.89	0.89	0.90	0.64	
	2020	0.67	0.93	0.89	0.90	0.79	
Sentinel 2	2016	0.53	0.69	0.33	0.53	0.69	0.50
	2018	0.50	0.81	0.67	0.50	0.81	
	2020	0.55	0.80	0.57	0.56	0.80	
Early Fusion	2016	0.40	0.76	0.67	0.95	0.69	0.66
	2018	0.67	0.93	0.91	0.92	0.81	
	2020	0.73	0.87	0.89	0.89	0.84	
Post classification composition	2016	0.53	0.86	0.89	0.93	0.69	0.67
	2018	0.62	0.85	0.91	0.92	0.76	
	2020	0.63	0.84	0.89	0.92	0.76	

As shown in Table 5, The accuracy of Sentinel 2 data-based classified maps achieved a low F1 score (<0.80) in a particular land cover class because clouds covered the study area that obscured the validation of land cover type behind clouds (Appendix 4). Regardless of misclassifications on Sentinel 2 classified maps, the FCN model performed well in mapping *natural forest class*, followed by *other land cover and water class* over methods on the other techniques that mostly achieved more than 0.80 of the F1 score. Meanwhile, the F1 score of the *oil palm* and *bare land class* barely exceed 0.80 in any techniques tested. It means that *oil palm* and *bare land class* appeared unreliable, as pixels were mostly misclassified as other land cover types (Appendix 4).

Nevertheless, this study was interested in a method that produced the best classification results over time. Because of this, comparing averaged F1 score is more preferred than the F1 score of each land cover class in Table 5. The Sentinel 2-based method also reached the lowest averaged F1 score, indicating clouds obscure validation of land cover type behind it. Otherwise, land cover classification results generated using

the post-classification composition technique reached the highest F1 score (0.67), showing a more substantial agreement with reality than the other methods. It also confirmed that their results were chosen for change detection. Figure 17 exhibits the post-classification composition classified maps of 2016, 2018, and 2020.



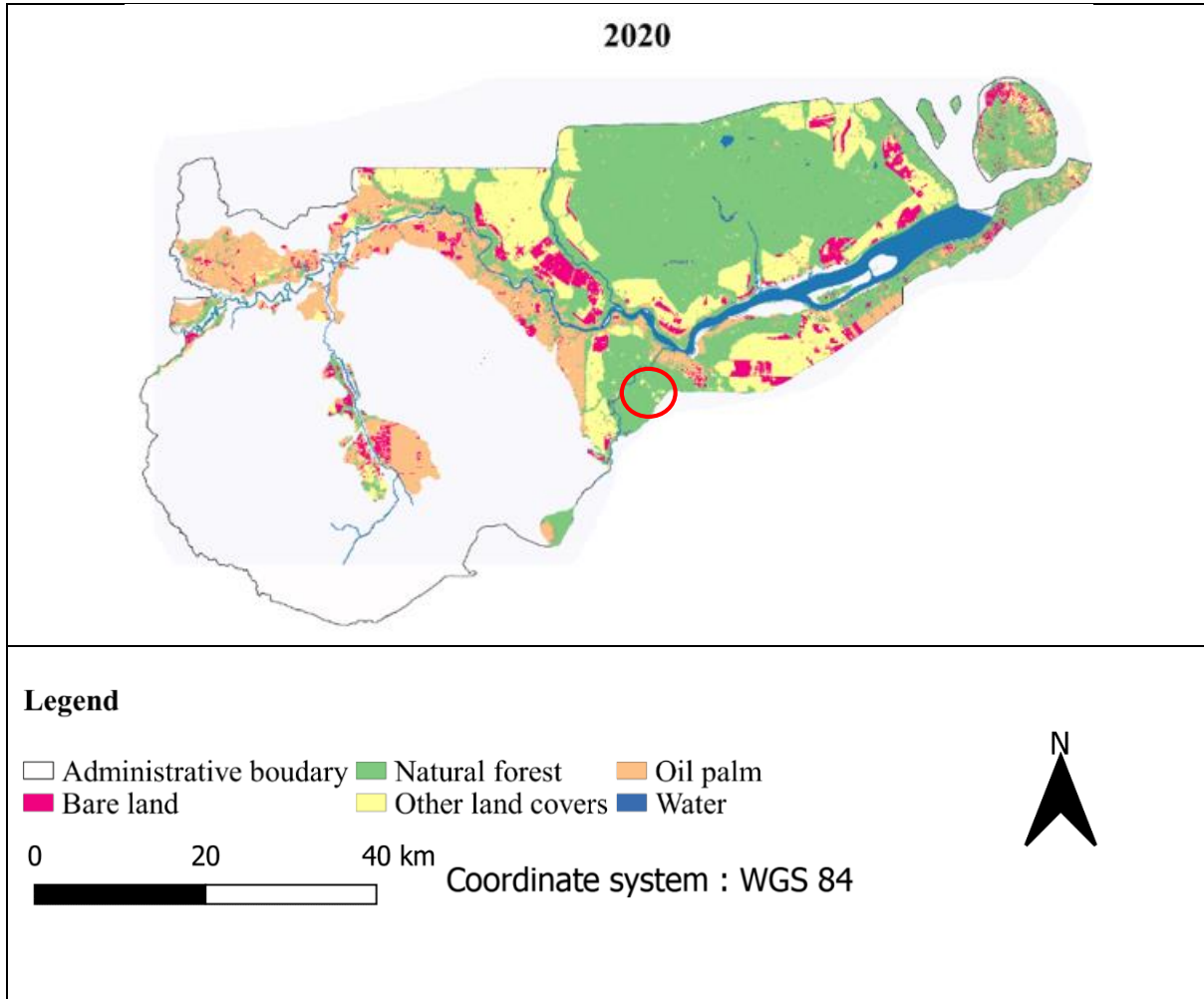


Figure 19. The classified land cover maps of 2016, 2018, and 2020 are based on post-classification composition technique. The red circle shows misclassifications associated with artefacts observed.

Figure 19 displays the post-classification composition classified map of 2016, 2018, and 2020. Based on visual inspection, artefacts (clouds and missing lines) were not entirely removed. Results revealed the misclassification of missing lines were apparent on the classified map of 2016. Clouds were misclassified on the classified map of 2018 and 2020. Moreover, most of them are exhibited in the natural forest area around peatlands, indicating the estimated size of natural forest looks like bias in peatlands.

3.4. The natural forest to oil palm conversions

As mentioned in the methodology section, the natural forest-to-oil palm conversion map was produced based on the chosen classified maps generated from the highest F1 score method (post-classification composition technique). The conversion map was produced using a post-classification approach. This procedure corresponds to before (from 2016 to 2018) and after the moratorium (from 2018 to 2020). Figure 20 shows the natural forest-to-oil palm conversion in both periods across the study area. In detail, Figures 20a and 20b show the distribution of the conversions in peatlands and riparian zones. Conversions in riparian zones elongated follow the river, whereas conversions were irregularly distributed in peatlands

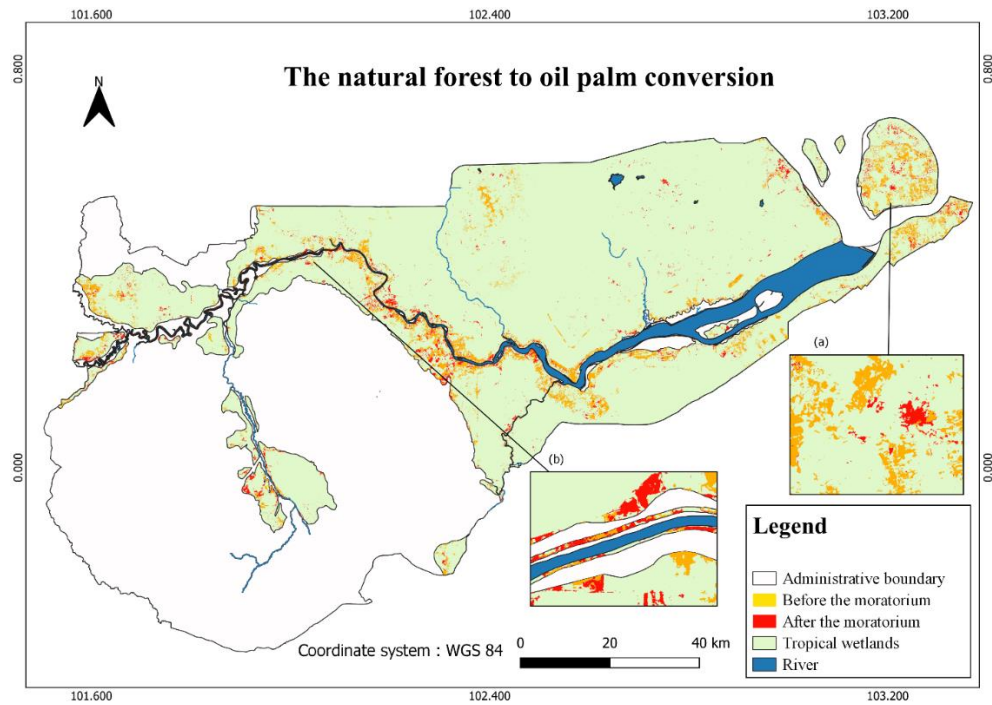


Figure 20. The natural forest to oil palm conversions map

For qualitative analysis, the number of locations is checked to understand to what extent the post-classification approach generated the natural forest to oil palm conversions map is real or unreal changes (misclassifications). Several conversions are identified as real (blue circle) and unreal (pink circle) changes. It indicates that correctly and incorrectly classified *natural forest* and *oil palm class* over time were compounded in the change map. Figure 21 and 22 portrays subsets of Planet imagery in the study area to identify real and unreal natural forest to oil palm changes before and after the moratorium period.



Figure 21. A subset of Planet imagery before the moratorium period (a) 2016, (b) 2018, (c) 2018 and conversion area classified. Blue circles observe real changes, whereas pink circles display unreal changes.

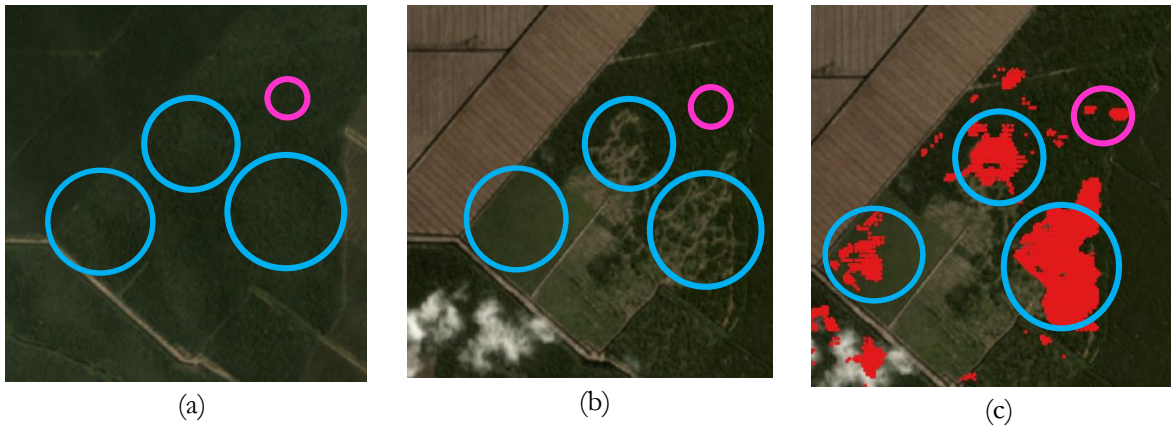


Figure 22. A subset of Planet imagery after the moratorium period (a) 2018, (b) 2020, (c) 2020 and conversion area classified. Blue circles observe real changes, whereas pink circles display unreal changes.

3.5. The impact of the moratorium in reducing the natural forest loss through oil palm expansion

This section evaluates the progress of the moratorium comparing before (2016-2018) and after the moratorium (2018-2020) in peatlands and riparian zones despite misclassification available. The difference between the classified natural forest and oil palm areas is presented through the absolute and percentage of loss and gain. The green/positive sign shows gain, and the red/negative sign shows a loss.

Table 6. The trend of natural forest areas

Tropical Wetlands	Total natural forest areas (ha)			Absolute loss/gain (ha)		Percentage loss/gain (%)	
	2016	2018	2020	2016 - 2018	2018 - 2020	2016 - 2018	2018 - 2020
Peatlands	344,675	321,314	342,846	-23,361	21,532	-6.78	6.70
Riparian zones	3,891	3,760	2,955	-131	-805	-3.37	-21.41

As shown in Table 6, the natural forest areas in both ecosystems decreased before the moratorium period (2016-2018). The percentage of natural forest loss in peatlands (-6.78%) was around two times higher than in riparian zones (-3.37%). However, the peat swamp forest was almost recovered after the moratorium. On the other hand, riparian forest intensively declined about around 21% after the moratorium period.

Table 7. The trend of oil palm areas

Tropical Wetlands	Total oil palm areas (ha)			Absolute loss/gain (ha)		Percentage loss/gain (%)	
	2016	2018	2020	2016-2018	2018-2020	2016-2018	2018-2020
Peatlands	102,858	137,495	112,863	34,637	-24,632	33.67	-17.91
Riparian zones	655	744	1,290	89	546	13.59	73.39

According to Table 7, oil palm areas increased before the moratorium period in peatlands (33.67%) and riparian zones (13.59%). However, after the moratorium, oil palm trees massively grew about 73 % in riparian zones. Meanwhile, the natural forest areas in peatlands declined about 18 % after the moratorium.

Table 8 provides a comprehensive result regarding natural forest to oil palm conversion issued in this study. In addition, the absolute and percentage of the conversions also are presented. Similar to the previous table, the green/positive sign shows gain, whereas the red/negative sign shows a loss.

Table 8. The trend of the conversions

Tropical Wetlands	Natural forest to oil palm (ha)		Absolute loss/gain (ha)	Percentage loss/gain (%)
	2016-2018	2018-2020		
Peatlands	29,980	11,694	-18,289	-61
Riparian zones	320	636	316	98.75

The natural forest loss driven by oil palm expansion decreased by about 61 % in peatlands, but it intensively increased nearly 99 % in riparian zones. These findings confirmed the difference of natural forest areas in both landscapes, as shown in Table 6. After the moratorium, the increase of 21,532 ha of natural forest areas replaced oil palm areas with about 18,289 ha in peatlands. Moreover, 316 ha of total natural forest loss in riparian zones (805 ha) was converted to oil palm areas. It concluded that the moratorium effectively reduced the natural forest conversion to oil palm areas in peatlands rather than in riparian zones.

4. DISCUSSION

In this chapter, Section 4.1-4.3, methods and results of land cover classification and change detection in this study are discussed. Section 4.4 discusses the moratorium's implication in reducing natural forest loss through oil palm expansion based on findings in this study. Section 4.5 findings are concluded to achieve research objectives and answer research questions. Section 4.6 recommended techniques are listed to improve this study in future works.

4.1. The importance of sampling design for land cover classification

A study conducted by Descals et al. (2019) mentioned that young oil palm plantations (<3 years old) in the Pelalawan Regency with minor canopy closure are available, whereas the mature oil palm plantations fully cover the surface in the study area through the field survey. Moreover, they also observed that people logged the natural forest areas. It may influence the quality of training samples that were collected using visual interpretation in this study. It did not consider the different ages between oil palm plantations and the disturbance of natural forests on the ground. It could be compensated if high-resolution imagery (e. g drone, Planet images) are available in the study area. However, it would also be a problem if the interpreter does not have experience in the study area. Therefore, the variation of physical characteristics (e. g canopy closure, ages, and level of disturbance) would be collected through a field survey to improve the quality of samples.

Besides the absence of a field survey, the low quality of samples may be caused by mixed pixels collected during samples collection. It is challenging for supervised classification to acquire highly separable training samples since this study used Sentinel imagery (10 m-spatial resolution). Lu et al. (2004) mentioned that satellite imagery pixels sometimes contain more than one land cover class. Pixels in training samples may have a mix of different land cover types, which is not representative. Spectral Mixture Analysis (SMA) could be applied prior to the training stage to improve the quality of samples. Mainly, the images would be transformed into fraction images to analyze Pixel Purity Index (PPI). It would be used to estimate the proportion of each pixel that is covered by a series of assigned land cover types. Pixels with 80-100% purity could be given as training samples of specific land cover types. Exploiting high-resolution imagery (e.g. Planet images) would also promising to avoid mixed pixels collected during samples collection. They have a higher spatial resolution so that land cover class captured would be more obvious than Sentinel imagery. As samples with mixed pixels are separated from pure pixels, the deep learning classifier could be trained well.

Sakti & Tsuyuki (2015) stated that accuracy shortcoming often occurs in heterogeneous land cover types, such as young plantations, burned peat, shrub, and the built-up area in the Pelalawan Regency. Using random sampling is inappropriate since the samples are generated randomly throughout the study area without controlling samples proportion. Stratified random sampling would be fit and manageable in large and heterogeneous areas, as Rocha et al. (2020) recommended. Large land cover classes would have more samples than small-area land cover classes. It is assumed large land cover classes having more diverse characteristics, which are needed to be captured, than smaller land cover classes. According to Appendix 3, the samples in this study may be distributed sequentially from large to small areas over time: 1) natural forest, 2) other land covers, 3) oil palm, and 4) bare land class if the stratified random sampling wants to be performed for further studies.

Samples collection within a patch size of 300 by 300 pixels is impracticable on Sentinel imagery. It was too large for generating samples in a large and heterogeneous area. Unrepresentative samples may be included within large patches. Then, generating smaller patches for samples collection would reduce unrepresentative samples collected, as long as the patch size is larger than the objects. Flood et al. (2019) employed a patch size of 128 by 128 pixels for land cover classification using the FCN model. Another alternative is to use points instead of polygon during samples collection. Sampling using points are manageable since the number of points represents the sample size. Meanwhile, the sample size is expressed as the polygon size when samples are collected based on polygons. Both recommendations may be tested to compare which technique would be the best to represent land cover types in a large and heterogeneous area.

4.2. The quality of land cover classification

This study observed that synergetic information between Sentinel imagery by early fusion and post-classification composition technique improved land cover classification accuracy. One of the problems observed is when Sentinel 1 and Sentinel 2 images were acquired on different dates. For instance, the Sentinel 1 images of 2016 were acquired in June 2016, while the Sentinel 2 images of 2016 were primarily acquired in September 2016 in this study (Appendix 1). The inconsistency of the acquisition date among Sentinel 1 and Sentinel 2 images issued images synchronicity (Christine Pohl, 2013). The issue also might appear at the tile level of Sentinel 1 and 2 images, as each image were mosaiced by tiles with a different date of acquisition (Appendix 1). Shortening the time difference among Sentinel 1 and 2 images and tiles may be an option to ensure the surface condition presented in both images is relatively the same.

Thick clouds are still a problem in both techniques. The results of the early fusion technique confirmed the findings by Bermudez et al. (2018) that spectral difference among the pixels of SAR and optical images caused a problem in removing thick clouds. To remove clouds, they also revealed a strategy to produce thin and thick clouds-free images, called Conditional Generative Adversarial Networks (cGAN). It mainly would remove clouds detected from Sentinel 2 imagery using Sentinel 1 images as auxiliary data through an adversarial scheme. Meraner et al. (2020) published residual learning for cloud removal (ResNet), which is derived from a super-resolution scheme, by integrating the information provided by Sentinel 1 and 2 images. In the future, researchers could test mentioned strategies before feeding them into the FCN model. Still, both strategies mentioned may be applicable if the date of acquisition between Sentinel 1 and Sentinel 2 imagery is close to avoid images desynchronization.

Meanwhile, cloud shadow detection on Sentinel 2 images are important in terms of the post-classification composition technique. This study observed small pixels associated with cloud shadow becoming misclassifications on Sentinel 2 classified maps. Although, pixels affected clouds should be classified thoroughly before being replaced by Sentinel 1 classified map. An operation that fully detects all types of clouds, especially cloud shadow, are necessary to avoid further misclassification when users apply the post-classification composition. Magno et al. (2021) introduced the AgroShadow tool to detect cloud shadow on Sentinel 2 images, consisting of several thresholds on reflectance ratio, indices, and k-mean classification algorithm. The mentioned operation may be included in the DeepGeo toolbox, developed by R. V. Mareto (2019) to improve cloud detection further.

The performance of the post-classification composition technique also relies on the accuracy of Sentinel 1 classified maps to fill the cloud pixels on Sentinel 2 classified maps. The accuracy of Sentinel 1 classified maps would be improved by adding additional bands in Sentinel 1 images. This study revealed that feeding only a dual-polarization band (VV-VH) to the FCN model misclassified *oil palm class* to the other land cover

types or vice versa over methods. Descals et al. (2019) demonstrated that adding texture information/Grey Level Co-occurrence Matrix (GLCM) to Sentinel 1 images could improve oil palm separability, natural forest, and built-up areas. Moreover, Ballester-berman & Rastoll-gimenez (2021) also suggested adding the VV/VH ratio band to distinguish between the *oil palm class* and the other land cover types. As a result, the model could extract more features of Sentinel 1 images by providing more bands to improve land cover types' discrepancy.

The proposed technique automatically produced higher overall accuracy than the land cover map of 2016 using visual interpretation by The Ministry of Agriculture of Indonesia (2016). It achieved 0.70 of overall accuracy, comparing to the post-classification composition classified map of 2016 reached 0.85 (Appendix 2). Descals et al. (2019) also mapped the natural forest and oil palm in Riau Province. They achieved an overall accuracy of approximately 0.90 in 2018 based on the fusion of S1 and S2 using a random forest classification. It was higher than our result produced in this study. They applied feature selection of S1 and S2 to filter redundant and non-informative data. Yet, this technique requires experts to choose the most relevant features. It could lead to an inaccurate prediction when experts wrongly select the features (DeLancey et al., 2020). Nevertheless, their technique could be applied in the circumstance of high-quality samples, and well-experienced experts are available. If both conditions are unavailable, users could test the deep learning and post-classification composition technique that this study revealed more than 80% of overall achieved in each classified map. Human intervention is only in the selection of training and test data and choosing optimal hyperparameters. The recommended technique (the post-classification composition technique) is also easily implemented since it only requires a GIS-practical approach.

4.3. The natural forest to oil palm change detection

Change detection in this study was derived from land cover classification produced using the FCN-based model (U-net). The constraint is that the FCN model only considers the spatial context of input images during the training process. Although, phenology patterns vary by vegetation type over time, which affects the signals or reflectance received by sensors (Rose & Nagle, 2021). It may cause misclassifications between vegetation classes in this study, such as *oil palm*, *natural forest*, and *other land cover class*. Constructing a model that could learn temporal dependencies or phenology patterns may improve land cover classification and then change detection. Ienco et al. (2019) proposed TWINNS (TWIN Neural Networks for Sentinel data) architecture to discover spatial and temporal dependencies of Sentinel imagery. By exploiting Convolutional Neural Networks (CNN) and Recurrent Neural Networks (RNN), the discriminative process of land cover types would be improved since the model look at the input images (Sentinel 1 and Sentinel 2) not only in a spatial context but also in a temporal context. Applying TWINNS may also enable the model to be trained with more features available. As a result, the high-accurate land cover classification may be achieved, as well as change detection.

A study conducted by Z. Zhu (2017) mentioned that the post-classification technique only identifies abrupt changes between dates. However, this technique is limited to a single-date approach to visualize abrupt changes within a study area. The information provided by post-classification change detection may be acceptable to visualize where conversions have taken place and the magnitude of changes. The trend and time of changes were not identified, which requires time series analysis. Verbesselt et al. (2010) developed The Breaks for Additive Season and Trend (BFAST) that iteratively decompose time series into trend, seasonal, remainder components for detecting changes. Reiche et al. (2015b) tested the capability of The Breaks for Additive Season and Trend (BFAST) and Landsat-SAR time series to detect natural forest change. They showed a satisfactory result, with the accuracies of fusion images remained high (0.95). Further studies

may test BFAST and Sentinel 1 and Sentinel 2 time series data to detect natural forest to oil palm conversion or vice versa to explore the technique and changes further.

4.4. The implication of the moratorium in reducing oil palm expansion in the natural forest area

The moratorium was enacted in 2018 to prevent natural forest loss through oil palm expansion. According to the map and change analysis produced in this study (Figure 20), the moratorium looks like it did not work as it should be. The conversions are seemed more intense in riparian zones than peatlands regardless of imperfection results generated. It does not mean the natural forest to oil palm changes in peatlands is neglected, as this study observed the natural forest to oil palm conversion in peatlands is larger than in riparian zones. It would generate an alarm to the Indonesian government that growers in tropical wetlands probably violated the moratorium. Appendix 5 also shows *other land cover*, and *bare land class* increased in peatlands or riparian zones that may be recommended for further research. The other stakeholders (e.g. certification institutions and NGOs) could track the land trajectory because change detection produced in this study is the "from-to" change map. It may be beneficial to avoid miss assessment and evaluate the moratorium's progress further. They also may adopt various methods based on their condition and shift from conventional to automated methods with various methods tested in this study.

Having the change map also shows the importance of transparent and up-to-date information. It may support in generating evidence-based decision making. Petrokofsky et al. (2011) mentioned that evidence-based decision making would be an asset to policymakers (Indonesia government). Policymakers enact decisions would be based on relevant studies that carefully describe the problem to define the best current evidence. The change map produced in this study could be used to give a broad understanding of natural forest to oil palm changes in the study area. Time series and change detection may support the findings further by providing evidence of the study area's magnitude, trend, and time of changes.

Nevertheless, the government has limited resources and requires collaborative efforts from various stakeholders to make evidence-based decision making happen. Researchers could help in improving methods to producing more robust and accurate change detection than before. Certification institutions and NGOs could disseminate results generated by researchers to growers and evaluate their sustainable practices in their plantations. Also, they could involve in the discussion, collect and validate information on the ground to be delivered to researchers and policymakers. If this strategy could be applied, sustainability in oil palm businesses would be achieved because the data is transparent and up-to-date between stakeholders. And thus, policymakers may enact further decisions based on better-informed evidence.

4.5. Conclusion

Land cover classification generated based on the synergy of Sentinel 1 and 2 data using the FCN model reached higher accuracy than single imagery results. Post classification composition technique (PCC) is more suitable than the early fusion technique (EF) for land cover classification as the PCC technique achieved a higher averaged F1 score than the EF technique. Besides the best technique mentioned achieving the highest accuracy, the recommended technique is practically easy to minimize cloud effects and reveal land cover types behinds clouds using the GIS-practical approach.

After the natural forest to oil palm changes map was generated, this study realizes that the spatial pattern of conversions is different in peatlands and riparian zones. The conversions in riparian zones elongated along

the river, while irregularly distributed conversions are observed in peatlands. Regardless of findings observed in this study, unreal changes mapped in some parts of the study area that would bias the information provided in the change map and need further improvement.

The moratorium looks like not effectively reduce the natural forest loss through oil palm expansion. Conversions in riparian zones seem more intense than in peatlands, whereas conversion area in peatlands also seems larger than in riparian zones. Besides providing information about the conversions in the study area, the results could be considered by different stakeholders involved to support evidence-based decision making. Therefore, the generation of further policies may be based on well-informed evidence driven by each stakeholder expertise.

4.6. Recommendation

List of recommendations for improving land cover classification and change detection in this study, as follows :

1. Implementing stratified random sampling to cope with the large and heterogeneous area of tropical wetlands.
2. Applying smaller size of patches to reduce unrepresentative samples collected.
3. Assigning samples by drawing points instead of polygons to manage the sample size.
4. Shortening the time difference at image-level and tile-level between Sentinel 1 and Sentinel 2 images before feeding into the model to avoid image desynchronization.
5. Shortening time difference between tiles of images before being mosaiced to reduce image desynchronization.
6. Conducting a field survey and inspecting the study area through high-resolution imagery (e.g. drone or Planet images) to differentiate the land cover types based on canopy coverage and level of natural forest disturbance.
7. Collecting *pure* pixels for samples collection by implementing Spectral Mixture Analysis (SMA) to obtain representative samples.
8. Applying an operation to fully detect clouds, including thin clouds, thick clouds, and cloud shadow, on Sentinel 2 images (e.g. AgrosShadow)
9. Adding additional bands of Sentinel 1 images (e.g. GLCM and VV/VH ratio) allow the model to extract the features further and increase the accuracy of the post-classification composition approach.
10. Applying noise removal techniques, such as cGAN or ResNet, to overcome cloud and missing lines issues when the early fusion technique wants to be performed.
11. Integrating BFAST and Synergy of sentinel 1 and 2 images to understand natural forest to oil palm changes further (e.g. the trend, and time of changes).
12. Applying the TWINNS model that would train the classifier in the spatial and temporal context together.
13. Collaborating with various stakeholders to improve change detection methods and data and support evidence-based decision making.

LIST OF REFERENCES

- Adeli, S., Salehi, B., Mahdianpari, M., Quackenbush, L. J., Brisco, B., Tamiminia, H., & Shaw, S. (2020). Wetland monitoring using SAR Data: A meta-analysis and comprehensive review. *Remote Sensing*, *12*(14). <https://doi.org/10.3390/rs12142190>
- Afriyanti, D., Hein, L., Kroeze, C., Zuhdi, M., & Saad, A. (2019). Scenarios for withdrawal of oil palm plantations from peatlands in Jambi Province, Sumatra, Indonesia. *Regional Environmental Change*, *19*(4), 1201–1215. <https://doi.org/10.1007/s10113-018-1452-1>
- Ballester-berman, J. D., & Rastoll-gimenez, M. (2021). *Sensitivity Analysis of Sentinel-1 Backscatter to Oil Palm Plantations at Pluriannual Scale : A Case Study in Gabon , Africa*. 1–22.
- Bermudez, J. D., Happ, P. N., Oliveira, D. A. B., & Feitosa, R. Q. (2018). SAR to OPTICAL IMAGE SYNTHESIS for CLOUD REMOVAL with GENERATIVE ADVERSARIAL NETWORKS. *ISPRS Annals of the Photogrammetry, Remote Sensing and Spatial Information Sciences*, *4*(1), 5–11. <https://doi.org/10.5194/isprs-annals-IV-1-5-2018>
- Chatziantoniou, A., Petropoulos, G. P., & Psomiadis, E. (2017). Co-Orbital Sentinel 1 and 2 for LULC mapping with emphasis on wetlands in a mediterranean setting based on machine learning. *Remote Sensing*, *9*(12). <https://doi.org/10.3390/rs9121259>
- Chellaiah, D., & Yule, C. M. (2018). Effect of riparian management on stream morphometry and water quality in oil palm plantations in Borneo. *Limnologia*, *69*(December 2017), 72–80. <https://doi.org/10.1016/j.limno.2017.11.007>
- Clerici, N., Valbuena Calderón, C. A., & Posada, J. M. (2017). Fusion of sentinel-1a and sentinel-2A data for land cover mapping: A case study in the lower Magdalena region, Colombia. *Journal of Maps*, *13*(2), 718–726. <https://doi.org/10.1080/17445647.2017.1372316>
- Close, O., Petit, S., Beaumont, B., & Hallot, E. (2021). *Analysis Associated to LULUCF in Wallonia , Belgium*.
- Dahiya, S., Garg, P. K., & Jat, M. K. (2013). A comparative study of various pixel-based image fusion techniques as applied to an urban environment. *International Journal of Image and Data Fusion*, *4*(3), 197–213. <https://doi.org/10.1080/19479832.2013.778335>
- DeLancey, E. R., Simms, J. F., Mahdianpari, M., Brisco, B., Mahoney, C., & Kariyeva, J. (2020). Comparing deep learning and shallow learning for large-scale wetland classification in Alberta, Canada. *Remote Sensing*, *12*(1). <https://doi.org/10.3390/RS12010002>
- Descals, A., Szantoi, Z., Meijaard, E., Sutikno, H., Rindanata, G., & Wich, S. (2019). Oil palm (*Elaeis guineensis*) mapping with details: Smallholder versus industrial plantations and their extent in riau, Sumatra. *Remote Sensing*, *11*(21). <https://doi.org/10.3390/rs11212590>
- Filipponi, F. (2019). Sentinel-1 GRD Preprocessing Workflow. *Proceedings*, *18*(1), 11. <https://doi.org/10.3390/ecrs-3-06201>
- Flood, N., Watson, F., & Collett, L. (2019). Using a U-net convolutional neural network to map woody vegetation extent from high resolution satellite imagery across Queensland, Australia. *International Journal of Applied Earth Observation and Geoinformation*, *82*(February), 101897. <https://doi.org/10.1016/j.jag.2019.101897>
- Gaveau, D. L. A., Sheil, D., Husnayaen, Salim, M. A., Arjasakusuma, S., Ancrenaz, M., ... Meijaard, E. (2016). Rapid conversions and avoided deforestation: Examining four decades of industrial plantation expansion in Borneo. *Scientific Reports*, *6*(September), 1–13. <https://doi.org/10.1038/srep32017>
- Graf, L., Bach, H., & Tiede, D. (2020). Semantic segmentation of sentinel-2 imagery for mapping irrigation center pivots. *Remote Sensing*, *12*(23), 1–19. <https://doi.org/10.3390/rs12233937>
- Gunawan, H. (2018). Indonesian peatland functions: Initiated peatland restoration and responsible management of peatland for the benefit of local community, case study in riau and west kalimantan provinces. In *Asia in Transition* (Vol. 7). https://doi.org/10.1007/978-981-10-8881-0_6
- Horton, A. J., Lazarus, E. D., Hales, T. C., Constantine, J. A., Bruford, M. W., & Goossens, B. (2018). Can Riparian Forest Buffers Increase Yields From Oil Palm Plantations? *Earth's Future*, *6*(8), 1082–1096. <https://doi.org/10.1029/2018EF000874>
- Ienco, D., Interdonato, R., Gaetano, R., & Ho Tong Minh, D. (2019). Combining Sentinel-1 and Sentinel-2 Satellite Image Time Series for land cover mapping via a multi-source deep learning architecture. *ISPRS Journal of Photogrammetry and Remote Sensing*, *158*(September), 11–22. <https://doi.org/10.1016/j.isprsjprs.2019.09.016>
- Jong, H. N. (2021, April 21). *Companies and officials flout forest-clearing moratorium in Papua, report finds*.

- Retrieved from <https://news.mongabay.com/2021/04/forest-peat-palm-oil-moratorium-papua-greenpeace-report/>
- Kementrian Pertanian Republik Indonesia. (2016). *Oil Palm Cover in Indonesia Oil Palm Cover*.
- Kolka, R. K., Murdiyarso, D., Kauffman, J. B., & Birdsey, R. A. (2016). Tropical wetlands, climate, and land-use change: adaptation and mitigation opportunities. *Wetlands Ecology and Management*, 24(2), 107–112. <https://doi.org/10.1007/s11273-016-9487-x>
- Li, W., Fu, H., Yu, L., & Cracknell, A. (2017). Deep learning based oil palm tree detection and counting for high-resolution remote sensing images. *Remote Sensing*, 9(1). <https://doi.org/10.3390/rs9010022>
- Lu, D., Mausel, P., Batistella, M., & Moran, E. (2004). Comparison of land-cover classification methods in the Brazilian Amazon basin. *Photogrammetric Engineering and Remote Sensing*, 70(6), 723–731. <https://doi.org/10.14358/PERS.70.6.723>
- Lyu, H., Lu, H., & Mou, L. (2016). Learning a transferable change rule from a recurrent neural network for land cover change detection. *Remote Sensing*, 8(6), 1–22. <https://doi.org/10.3390/rs8060506>
- Magno, R., Rocchi, L., Dainelli, R., Matese, A., Gennaro, S. F. Di, Chen, C. F., ... Toscano, P. (2021). Agroshadow: A new sentinel-2 cloud shadow detection tool for precision agriculture. *Remote Sensing*, 13(6), 1–11. <https://doi.org/10.3390/rs13061219>
- Makinde, E. O., & Oyelade, E. O. (2020). Land cover mapping using Sentinel-1 SAR and Landsat 8 imageries of Lagos State for 2017. *Environmental Science and Pollution Research*, 27(1), 66–74. <https://doi.org/10.1007/s11356-019-05589-x>
- Maretto, R. V. (2020). AUTOMATING LAND COVER CHANGE DETECTION : A DEEP LEARNING BASED APPROACH TO MAP Doctorate Thesis of the Graduate Course in Applied Computing , guided by Drs . Leila Maria Garcia Fonseca , and Thales Sehn Körting , approved in March 20 , 2020 . *Instituto Nacional de Pesquisas Espaciais - INPE*, 109. Retrieved from <http://urlib.net/8JMKD3MGP3W34R/42L55PP>
- Maretto, R. V. (2019). *AN EXTENSIBLE AND EASY-TO-USE TOOLBOX FOR DEEP LEARNING BASED ANALYSIS OF REMOTE SENSING IMAGES* Raian Vargas Maretto , Thales Sehn Körting , Leila Maria Garcia Fonseca. 9815–9818.
- Maretto, R. V., Fonseca, L. M. G., Jacobs, N., Korting, T. S., Bendini, H. N., & Parente, L. L. (2020). Spatio-Temporal Deep Learning Approach to Map Deforestation in Amazon Rainforest. *IEEE Geoscience and Remote Sensing Letters*, 1–5. <https://doi.org/10.1109/lgrs.2020.2986407>
- Meraner, A., Ebel, P., Zhu, X. X., & Schmitt, M. (2020). Cloud removal in Sentinel-2 imagery using a deep residual neural network and SAR-optical data fusion. *ISPRS Journal of Photogrammetry and Remote Sensing*, 166, 333–346. <https://doi.org/10.1016/J.ISPRSJPRS.2020.05.013>
- Ministry of Environmental and Forestry, I. (2017). The Guideline to Monitor Land Cover Types.
- Parente, L., Taquary, E., Silva, A. P., Souza, C., & Ferreira, L. (2019). Next generation mapping: Combining deep learning, cloud computing, and big remote sensing data. *Remote Sensing*, 11(23). <https://doi.org/10.3390/rs11232881>
- Petrokofsky, G., Holmgren, P., & Brown, N. D. (2011). Reliable forest carbon monitoring - Systematic reviews as a tool for validating the knowledge base. *International Forestry Review*, 13(1), 56–66. <https://doi.org/10.1505/ifor.13.1.56>
- Phan, T. H., & Yamamoto, K. (2020). *Resolving Class Imbalance in Object Detection with Weighted Cross Entropy Losses*. Retrieved from <http://arxiv.org/abs/2006.01413>
- Planet. (2020). Planet QGIS Plugin. Retrieved August 3, 2021, from <https://developers.planet.com/docs/integrations/qgis/>
- Pohl, C., & Van Genderen, J. L. (1998). Review article Multisensor image fusion in remote sensing: Concepts, methods and applications. In *International Journal of Remote Sensing* (Vol. 19). <https://doi.org/10.1080/014311698215748>
- Pohl, Christine. (2013). Challenges of Remote Sensing Image Fusion to Optimize Earth Observation Data Exploration. *European Scientific Journal*, 4(December), 355–365. Retrieved from <http://ejournal.org/index.php/esj/article/download/2487/2360>
- Reiche, J., Verbesselt, J., Hoekman, D., & Herold, M. (2015a). Fusing Landsat and SAR time series to detect deforestation in the tropics. *Remote Sensing of Environment*, 156, 276–293. <https://doi.org/10.1016/j.rse.2014.10.001>
- Reiche, J., Verbesselt, J., Hoekman, D., & Herold, M. (2015b). Fusing Landsat and SAR time series to detect deforestation in the tropics. *Remote Sensing of Environment*, 156, 276–293. <https://doi.org/10.1016/j.rse.2014.10.001>
- Rose, M. B., & Nagle, N. N. (2021). Characterizing forest dynamics with landsat-derived phenology

- curves. *Remote Sensing*, 13(2), 1–21. <https://doi.org/10.3390/rs13020267>
- RSPO. (2018). *Roundtable on Sustainable Palm Oil-principles and criteria*. 137. Retrieved from http://www.rspo.org/file/RSPO_P&C2013_with_Major_Indicators_Endorsed_by_BOG_FINAL_A5_25thApril2014.pdf
- Ruysschaert, D., & Salles, D. (2014). Towards global voluntary standards: Questioning the effectiveness in attaining conservation goals. The case of the Roundtable on Sustainable Palm Oil (RSPO). *Ecological Economics*, 107, 438–446. <https://doi.org/10.1016/j.ecolecon.2014.09.016>
- Sakti, A. D., & Tsuyuki, S. (2015). Spectral mixture analysis (SMA) of Landsat imagery for land cover study of highly degraded peatland in Indonesia. *International Archives of the Photogrammetry, Remote Sensing and Spatial Information Sciences - ISPRS Archives*, 40(7W3), 495–501. <https://doi.org/10.5194/isprsarchives-XL-7-W3-495-2015>
- Sefrin, O., Riese, F. M., & Keller, S. (2021). Deep learning for land cover change detection. *Remote Sensing*, 13(1), 1–27. <https://doi.org/10.3390/rs13010078>
- Spruce, J., Bolten, J., Mohammed, I. N., Srinivasan, R., & Lakshmi, V. (2020). Mapping Land Use Land Cover Change in the Lower Mekong Basin From 1997 to 2010. *Frontiers in Environmental Science*, 8(March). <https://doi.org/10.3389/fenvs.2020.00021>
- Steinhausen, M. J., Wagner, P. D., Narasimhan, B., & Waske, B. (2018). Combining Sentinel-1 and Sentinel-2 data for improved land use and land cover mapping of monsoon regions. *International Journal of Applied Earth Observation and Geoinformation*, 73, 595–604. <https://doi.org/10.1016/j.jag.2018.08.011>
- Suleiman, M. S., Wasonga, O. V., Mbau, J. S., & Elhadi, Y. A. (2017). Spatial and temporal analysis of forest cover change in Falgore Game Reserve in Kano, Nigeria. *Ecological Processes*, 6(1). <https://doi.org/10.1186/s13717-017-0078-4>
- Thakkar, A. K., Desai, V. R., Patel, A., & Potdar, M. B. (2017). Post-classification corrections in improving the classification of Land Use/Land Cover of arid region using RS and GIS: The case of Arjuni watershed, Gujarat, India. *The Egyptian Journal of Remote Sensing and Space Science*, 20(1), 79–89. <https://doi.org/10.1016/J.EJRS.2016.11.006>
- Verbesselt, J., Hyndman, R., Newnham, G., & Culvenor, D. (2010). Detecting trend and seasonal changes in satellite image time series. *Remote Sensing of Environment*, 114(1), 106–115. <https://doi.org/10.1016/j.rse.2009.08.014>
- Yan, Y., Tan, Z., & Su, N. (2019). A data augmentation strategy based on simulated samples for ship detection in RGB remote sensing images. *ISPRS International Journal of Geo-Information*, 8(6). <https://doi.org/10.3390/ijgi8060276>
- Ying, X. (2019). An Overview of Overfitting and its Solutions. *Journal of Physics: Conference Series*, 1168(2). <https://doi.org/10.1088/1742-6596/1168/2/022022>
- You, K., Long, M., Wang, J., & Jordan, M. I. (2019). *How Does Learning Rate Decay Help Modern Neural Networks?* Retrieved from <http://arxiv.org/abs/1908.01878>
- Yustiawati, Sazawa, K., Syawal, M. S., Kuramitz, H., Saito, T., Hosokawa, T., ... Tanaka, S. (2015). Peat fire impact on water quality and organic matter in peat soil. In *Tropical Peatland Ecosystems*. https://doi.org/10.1007/978-4-431-55681-7_18
- Yusuf, A. A., & Roos, E. L. (2017). Indonesia's Moratorium on Palm Oil Expansion from Natural Forest: Economy-Wide Impact and the Role of International Transfers CoPS Working Paper No. G-276, September 2017 Centre of Policy Studies, Victoria University. *Asian Development Review*, 35(2), 85–112.
- Zhang, C., Atkinson, P. M., George, C., Wen, Z., Diazgranados, M., & Gerard, F. (2020). ISPRS Journal of Photogrammetry and Remote Sensing Identifying and mapping individual plants in a highly diverse high-elevation ecosystem using UAV imagery and deep learning. *ISPRS Journal of Photogrammetry and Remote Sensing*, 169(October), 280–291. <https://doi.org/10.1016/j.isprsjprs.2020.09.025>
- Zhu, X. X., Tuia, D., Mou, L., Xia, G.-S., Zhang, L., Xu, F., & Fraundorfer, F. (2017). *Deep learning in remote sensing: a review*. (December). <https://doi.org/10.1109/MGRS.2017.2762307>
- Zhu, Z. (2017). Change detection using landsat time series: A review of frequencies, preprocessing, algorithms, and applications. *ISPRS Journal of Photogrammetry and Remote Sensing*, 130, 370–384. <https://doi.org/10.1016/J.ISPRSJPRS.2017.06.013>
- Zhuang, J., Yang, J., Gu, L., & Dvornek, N. (2019). Shelfnet for fast semantic segmentation. *Proceedings - 2019 International Conference on Computer Vision Workshop, ICCVW 2019*, 847–856. <https://doi.org/10.1109/ICCVW.2019.00113>

APPENDICES

1. Date of Acquisition

a. Sentinel 1

Year	Number of tiles	Date of Acquisition
2016	5	19 July 2016
		19 July 2016
		19 July 2016
		26 July 2016
		26 July 2016
2018	5	9 July 2018
		16 July 2018
		21 July 2018
		28 July 2018
		28 July 2018
2020	5	28 June 2020
		10 July 2020
		10 July 2020
		17 July 2020
		17 July 2020

b. Sentinel 2

Year	Number of tiles	Date of acquisition
2016	9	19 May 2016
		7 Agustus 2016
		7 Agustus 2016
		3 September 2016
		3 September 2016
		3 September 2016
		3 September 2016
		3 September 2016
		3 September 2016
2018	9	3 June 2018
		10 June 2018
		30 June 2018
		5 July 2018
		5 July 2018

Year	Number of tiles	Date of acquisition
		5 July 2018
		5 July 2018
		12 August 2018
		13 September 2018
2020	9	30 May 2020
		2 July 2020
		7 July 2020
		28 August 2020
		28 August 2020
		22 September 2020
		1 October 2020
		2 October 2020
		2 October 2020

2. Confusion matrix of Sentinel 2 classified maps of 2016 during hyperparameters tuning Set C

Classified	Reference							
	Land cover class	cloud	bare land	natural forest	other land cover	oil palm	water	Total
	cloud	0	2	13	11	4	5	35
	bare land	0	4	0	0	3	0	7
	natural forest	0	0	58	0	4	0	63
	other land cover	0	1	2	20	1	0	23
	oil palm	0	1	2	3	15	0	21
	water	0	0	1	0	0	0	1
	Total	0	8	76	34	27	5	150

Set D

Classified	Reference							
	Land cover class	cloud	bare land	natural forest	other land cover	oil palm	water	Total
	cloud	0	2	13	11	5	4	35
	bare land	0	4	0	0	2	0	6
	natural forest	0	0	58	1	5	0	64
	other land cover	0	1	2	19	0	0	22
	oil palm	0	1	3	3	15	0	22
	water	0	0	0	0	0	1	1
	Total	0	8	76	34	27	5	150

Set E

Classified	Reference							
	Land cover class	cloud	bare land	natural forest	other land covers	oil palm	water	Total
	cloud	0	2	13	11	5	4	35
	bare land	0	4	0	0	3	0	7
	natural forest	0	0	60	1	4	0	65
	other land covers	0	2	0	19	0	0	21
	oil palm	0	0	3	3	15	0	21
	water	0	0	0	0	0	1	1
	Total	0	8	76	34	27	5	150

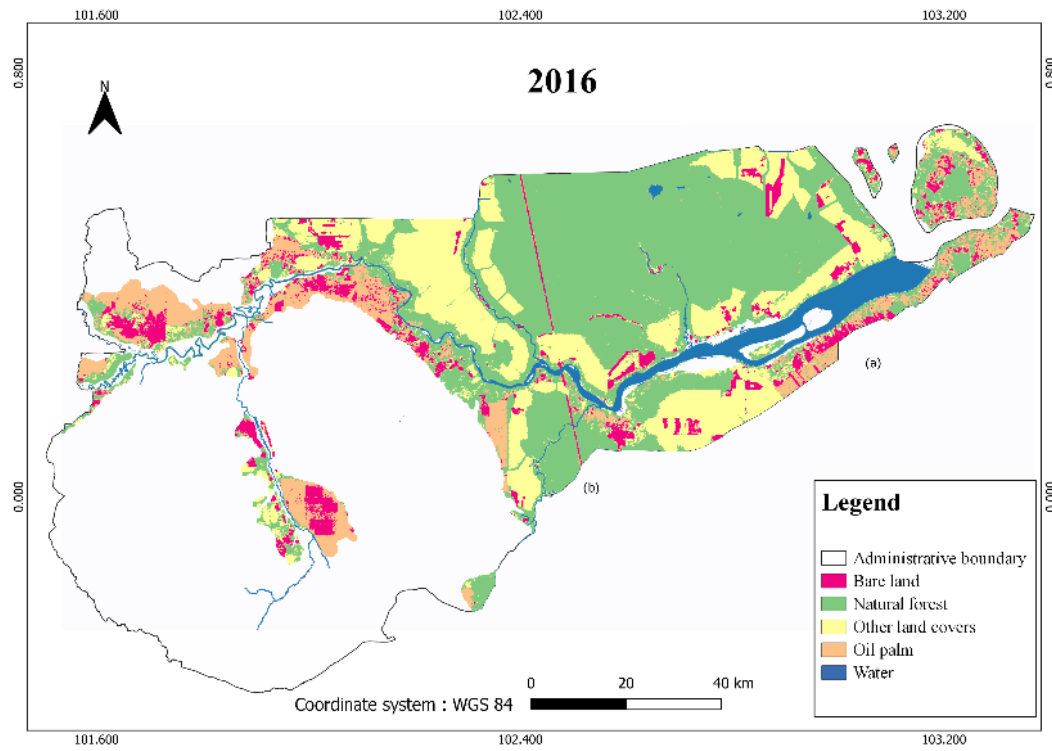
3. After Implementing the best hyperparameters over methods over time

Dataset	Year	Overall Accuracy
Sentinel 1	2016	0.81
	2018	0.83
	2020	0.87
Sentinel 2	2016	0.66
	2018	0.78
	2020	0.71
Early Fusion	2016	0.81
	2018	0.89
	2020	0.87
Post classification composition	2016	0.85
	2018	0.86
	2020	0.85

4. Land cover classification

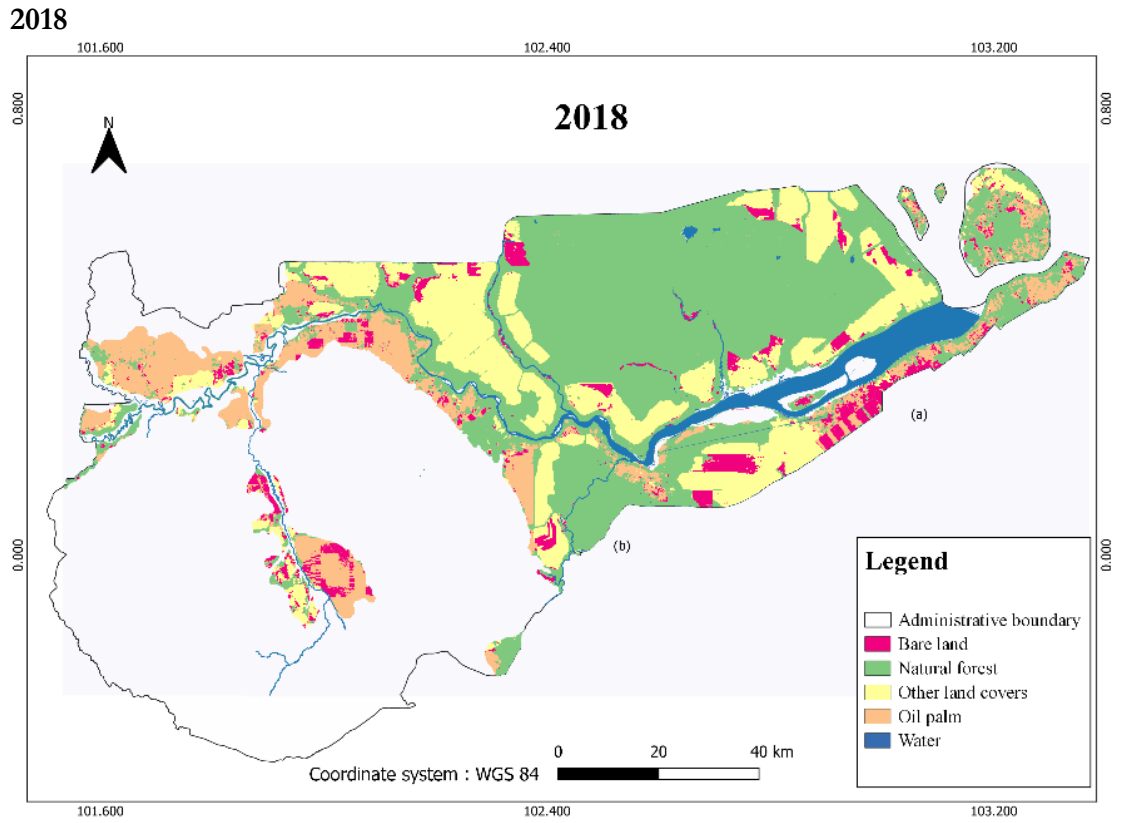
a. Sentinel 1 (S1)

2016



Confusion matrix of S1 2016

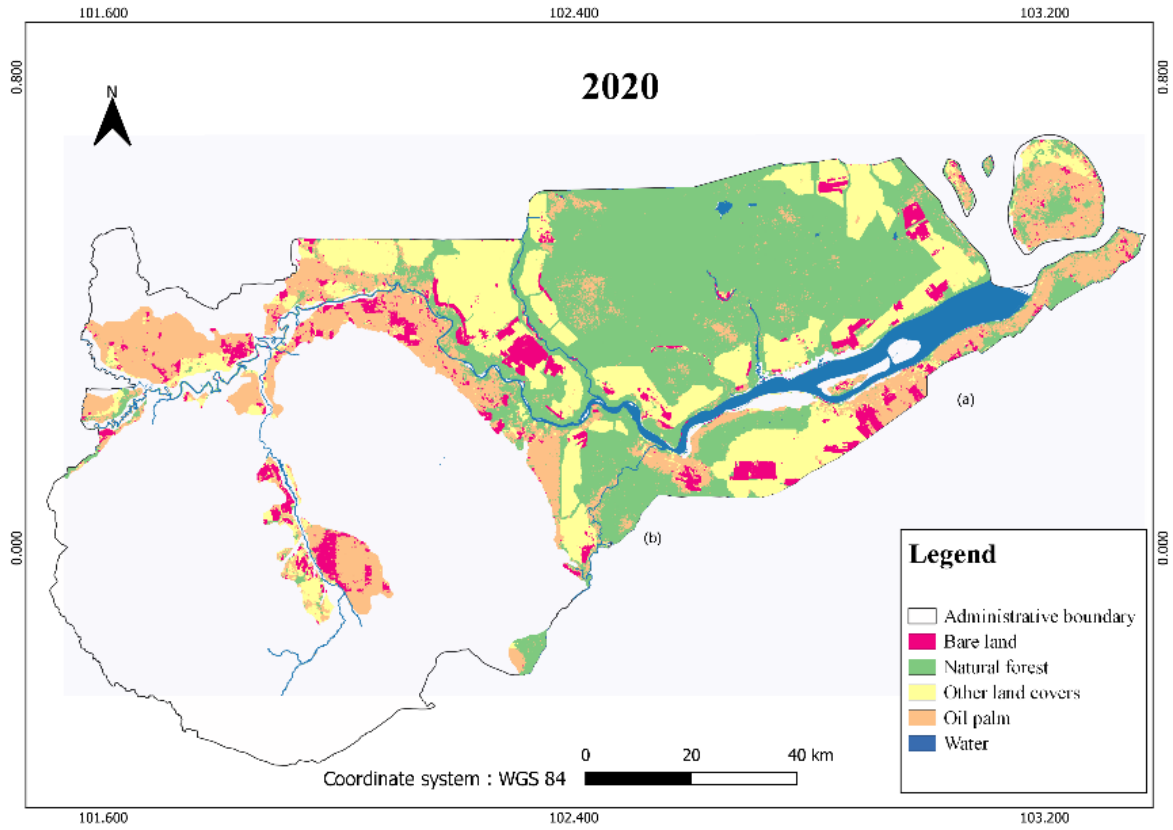
Predicted	Reference						Total
	Land cover class	bare land	natural forest	other land covers	oil palm	water	
bare land		4	1	2	5	0	12
natural forest		0	69	2	4	2	77
other land covers		3	5	29	2	0	39
oil palm		1	1	1	16	0	19
water		0	0	0	0	3	3
Total		8	76	34	27	5	150



Confusion matrix of S1 2018

Predicted	Reference						Total
	Land cover class	bare land	natural forest	other land covers	oil palm	water	
bare land	2	1	1	3	0	7	
natural forest	0	71	2	8	1	82	
other land covers	1	1	32	2	0	36	
oil palm	2	2	1	16	0	21	
water	0	0	0	0	4	4	
Total	5	75	36	29	5	150	

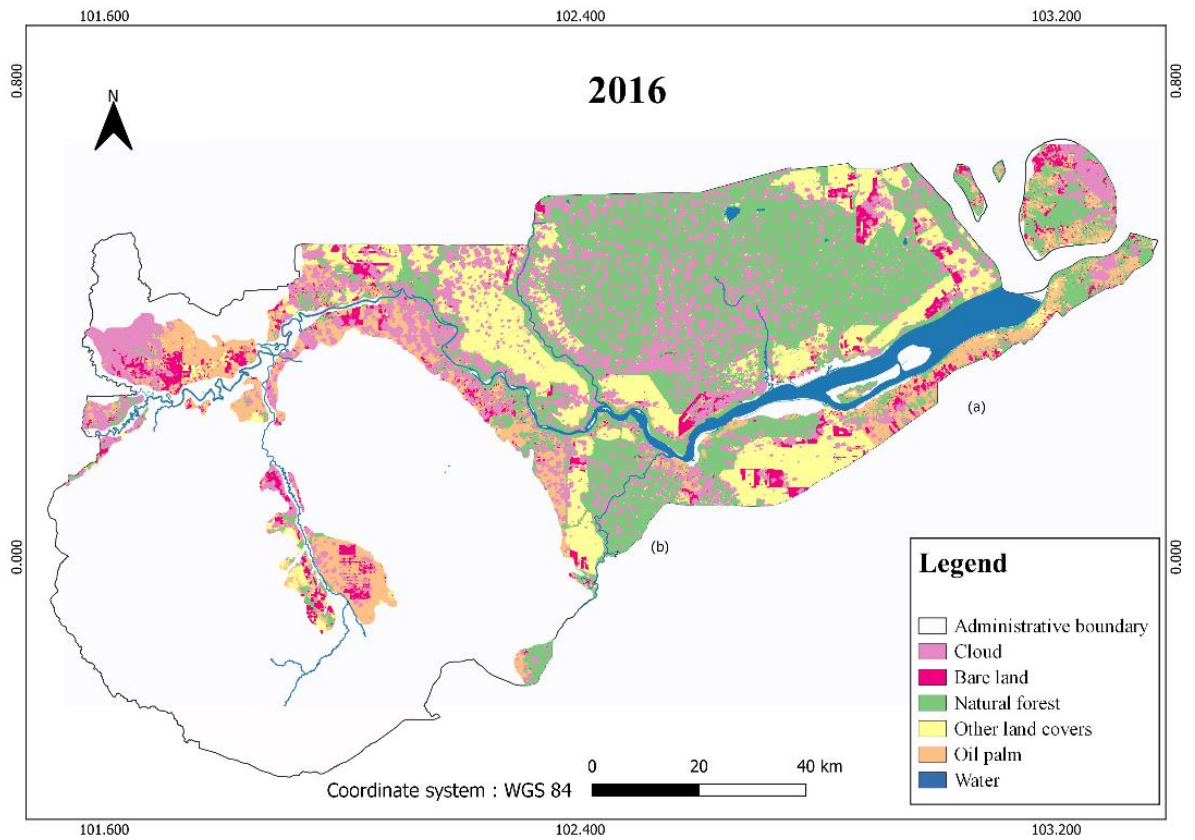
2020



Confusion matrix of S1 2020

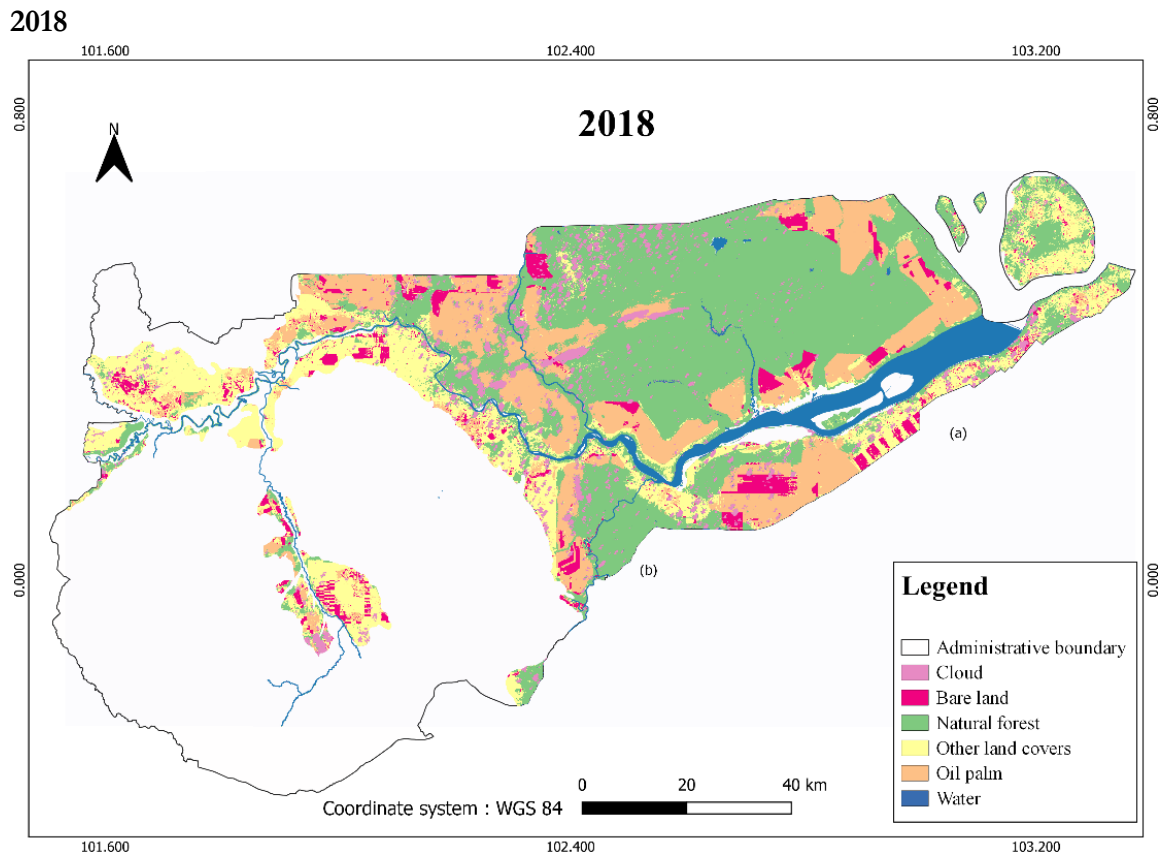
Predicted	Land cover class	Reference					Total
		bare land	natural forest	other land covers	oil palm	water	
	bare land	5	1	0	2	0	8
	natural forest	0	64	2	1	0	67
	other land cover	1	2	33	0	0	36
	oil palm	1	8	0	25	1	35
	water	0	0	0	0	4	4
	Total	7	75	35	28	5	150

**b. Sentinel 2 (S2)
2016**



Confusion matrix of S2 2016

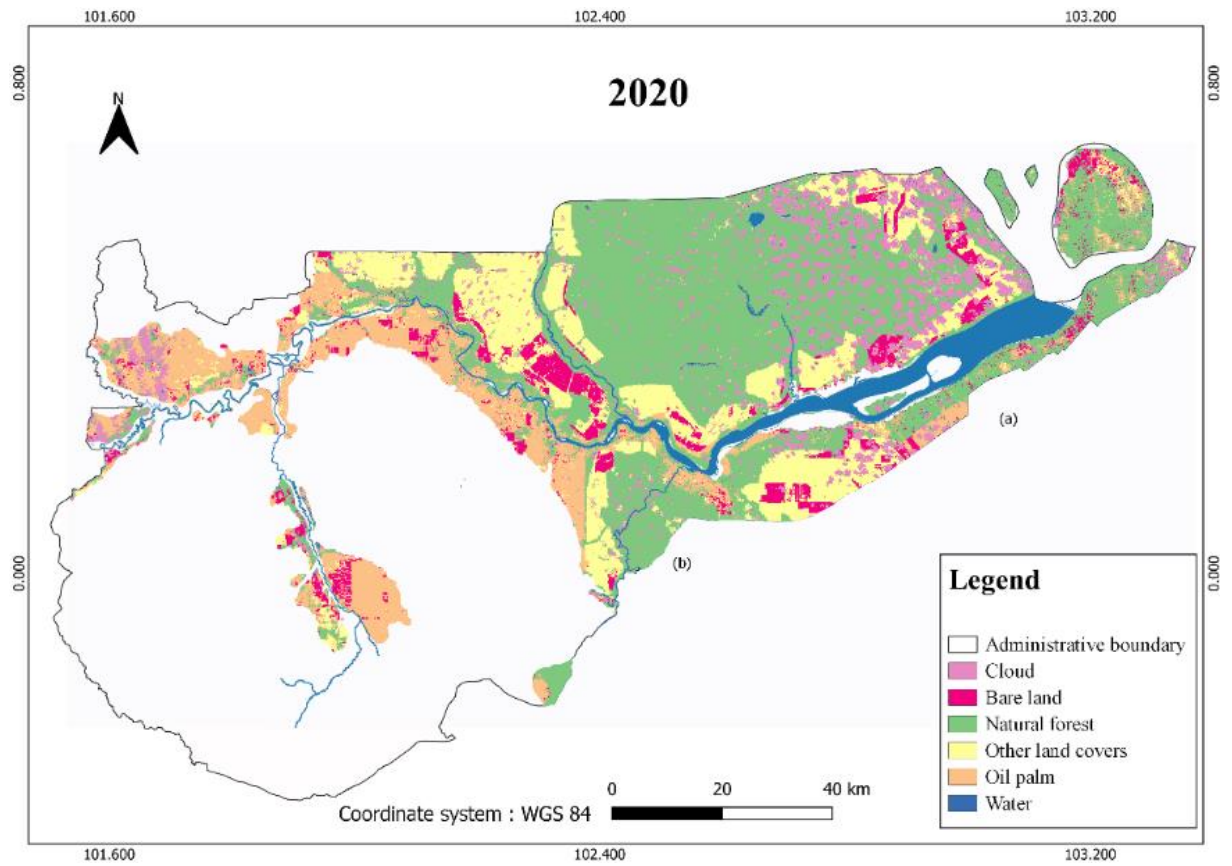
Classified	Land cover class	Reference						Total
		cloud	bare land	natural forest	other land covers	oil palm	water	
	cloud	0	2	13	11	5	4	35
	bare land	0	4	0	0	3	0	7
	natural forest	0	0	60	1	4	0	65
	other land covers	0	2	0	19	0	0	21
	oil palm	0	0	3	3	15	0	21
	water	0	0	0	0	0	1	1
	Total	0	8	76	34	27	5	150



Confusion matrix of S2 2018

Classified	Land cover class	Reference						Total
		cloud	bare land	natural forest	other land covers	oil palm	water	
	cloud	0	2	4	3	4	2	15
	bare land	0	3	1	2	1	0	7
	natural forest	0	0	64	2	2	0	68
	other land covers	0	0	3	28	2	0	33
	oil palm	0	0	3	1	19	0	23
	water	0	0	0	0	1	3	4
	Total	0	5	75	36	29	5	150

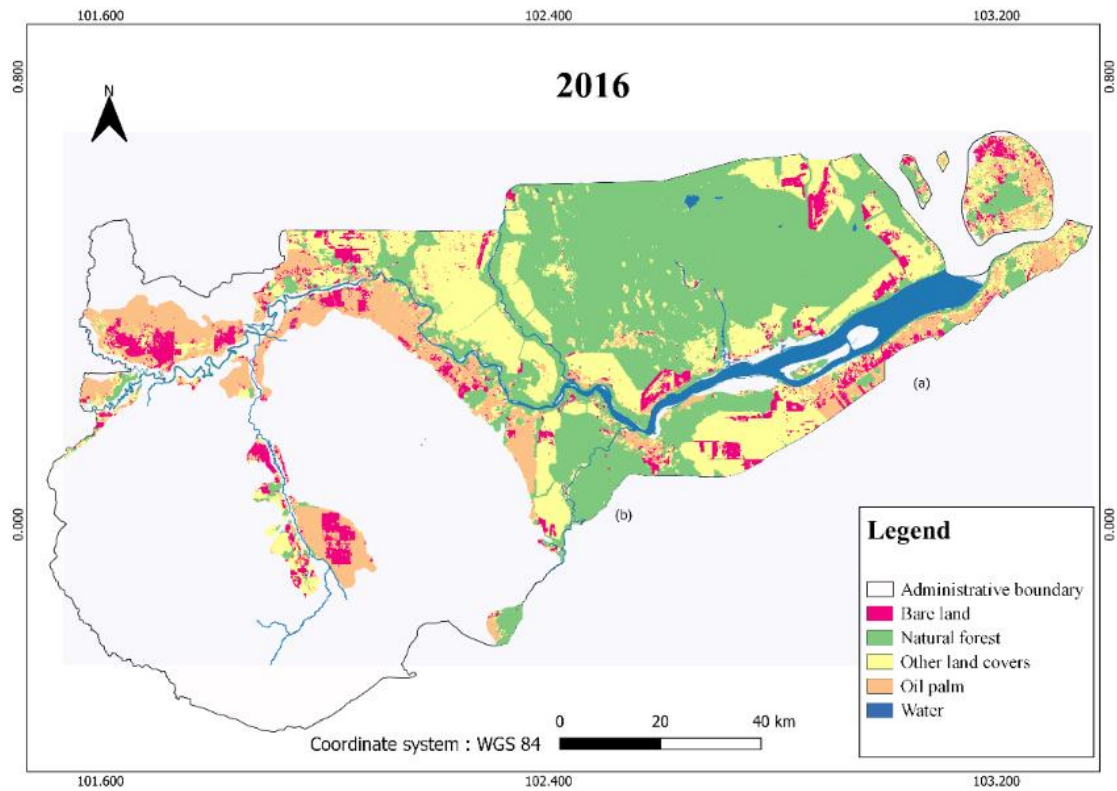
2020



Confusion matrix of S2 2020

Classified	Reference							
	Land cover class	cloud	bare land	natural forest	other land covers	oil palm	water	Total
cloud	0	1	16	2	2	3	24	
bare land	0	5	1	4	1	0	11	
natural forest	0	0	54	2	4	0	60	
other land covers	0	1	1	26	2	0	30	
oil palm	0	0	3	1	19	0	23	
water	0	0	0	0	0	2	2	
Total	0	7	75	35	28	5	150	

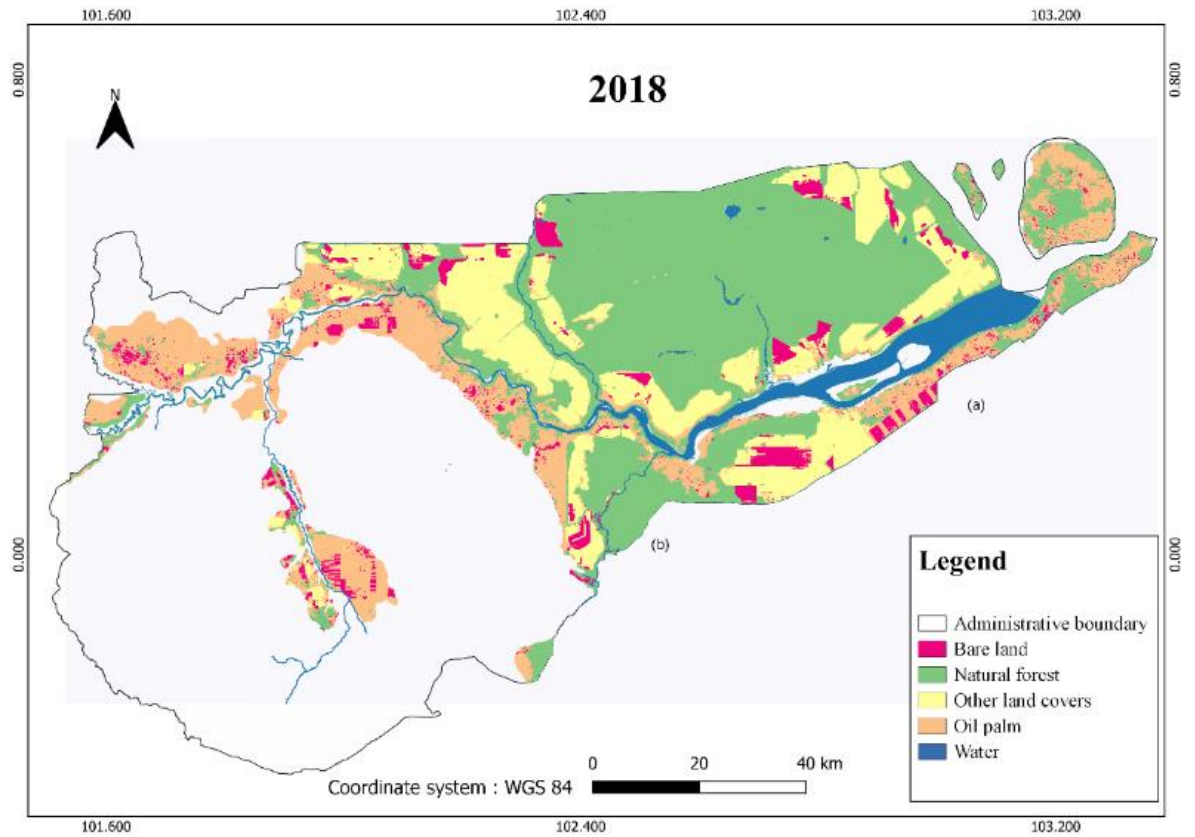
c. Early Fusion (EF)
2016



Confusion matrix of EF 2016

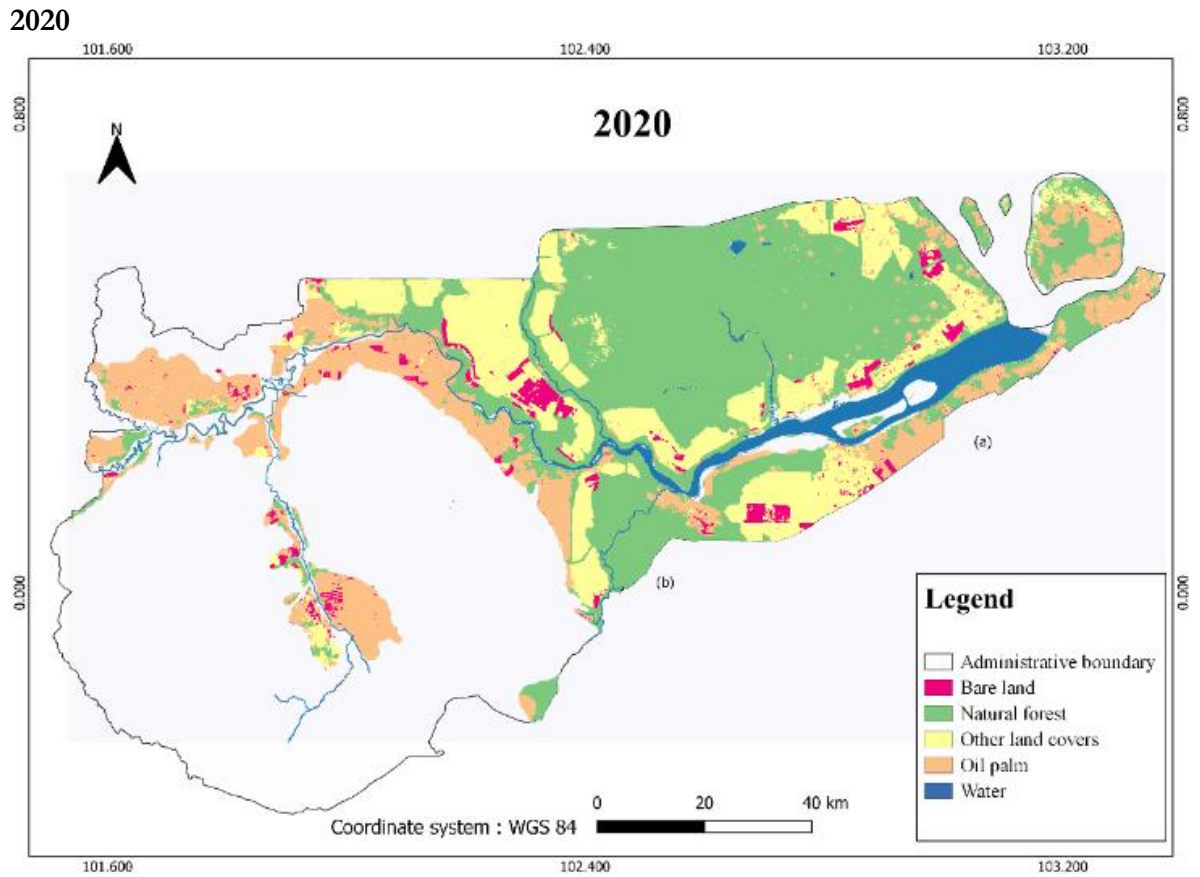
Predicted	Land cover class	Reference					Total
		bare land	natural forest	other land covers	oil palm	water	
	bare land	4	0	3	4	1	12
	natural forest	0	69	0	0	1	70
	other land covers	3	5	29	5	0	42
	oil palm	1	2	2	17	0	22
	water	0	0	0	1	3	4
	Total	8	76	34	27	5	150

2018



Confusion matrix of EF 2018

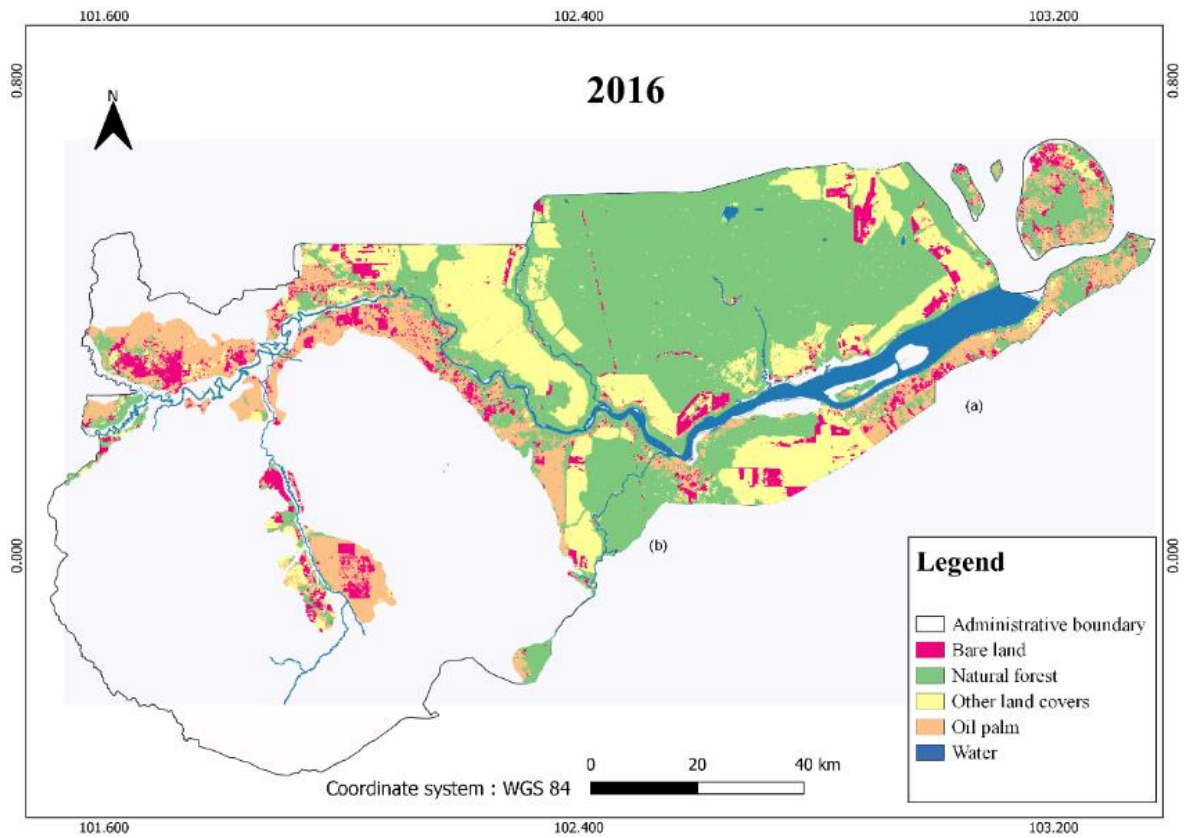
Predicted	Reference						Total
	Land cover class	bare land	natural forest	other land covers	oil palm	water	
bare land		4	1	1	1	0	7
natural forest		1	69	2	3	0	75
other land covers		0	0	31	0	0	31
oil palm		0	4	2	24	0	30
water		0	1	0	1	5	7
Total		5	75	36	29	5	150



Confusion matrix of EF 2020

Predicted	Land cover class	Reference					Total
		bare land	natural forest	other land covers	oil palm	water	
	bare land	4	0	0	0	0	4
	natural forest	0	63	2	2	0	67
	other land covers	2	6	33	0	0	41
	oil palm	1	6	0	26	1	34
	water	0	0	0	0	4	4
	Total	7	75	35	28	5	150

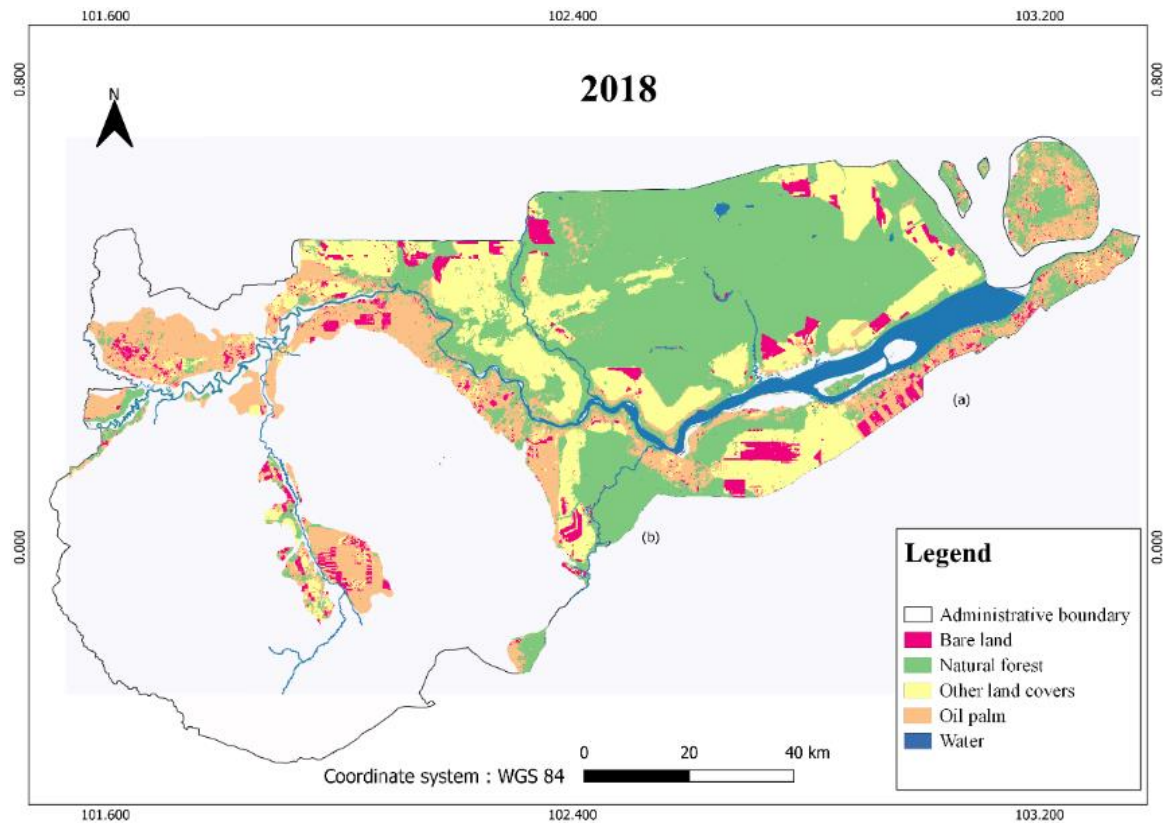
**d. Post classification composition (PCC)
2016**



Confusion matrix of PCC 2016

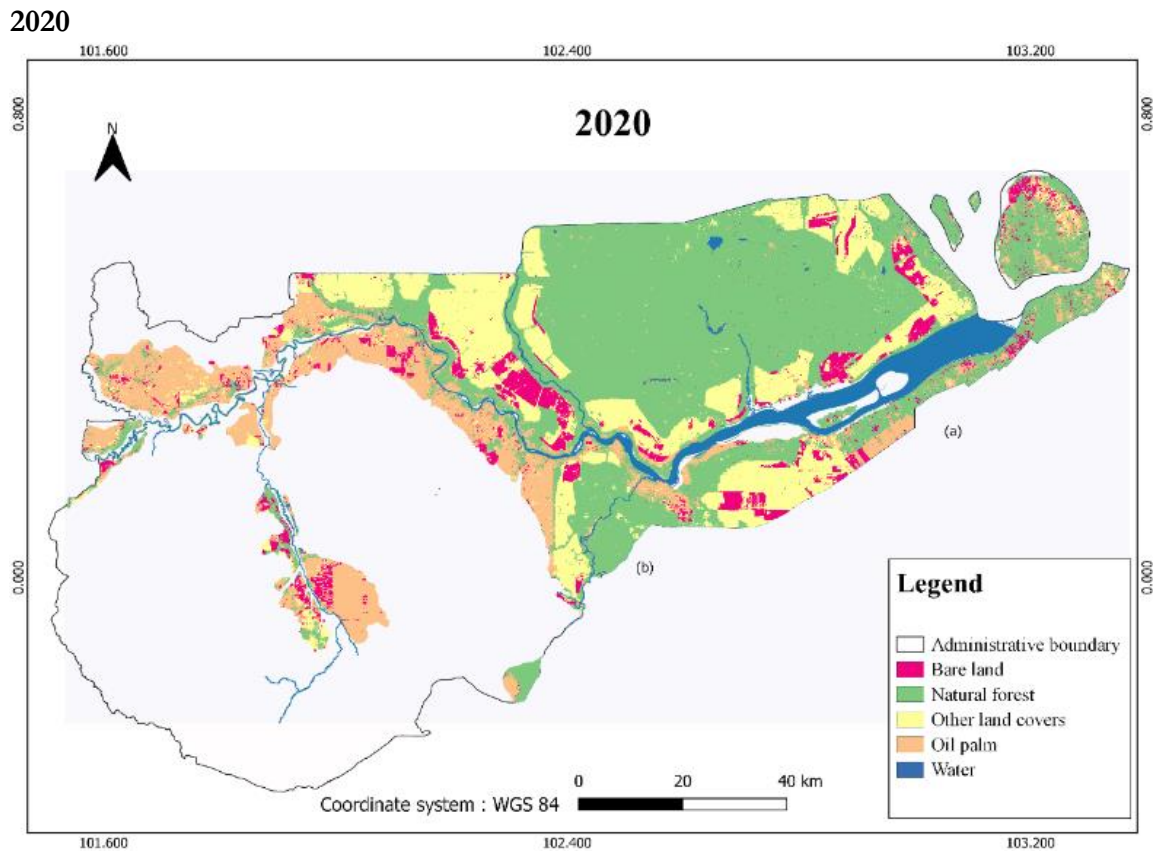
	Reference						Total
	Land cover class	bare land	natural forest	other land covers	oil palm	water	
Predicted	bare land	5	0	2	4	0	11
	natural forest	0	73	2	5	1	81
	other land covers	2	0	27	0	0	29
	oil palm	1	3	3	18	0	25
	water	0	0	0	0	4	4
	Total	8	76	34	27	5	150

2018



Confusion matrix of PCC 2018

Predicted	Reference						
	Land cover class	bare land	natural forest	other land covers	oil palm	water	Total
bare land		4	1	2	1	0	8
natural forest		0	68	2	3	0	73
other land covers		0	3	31	3	0	37
oil palm		1	3	1	21	0	26
water		0	0	0	1	5	6
Total		5	75	36	29	5	150



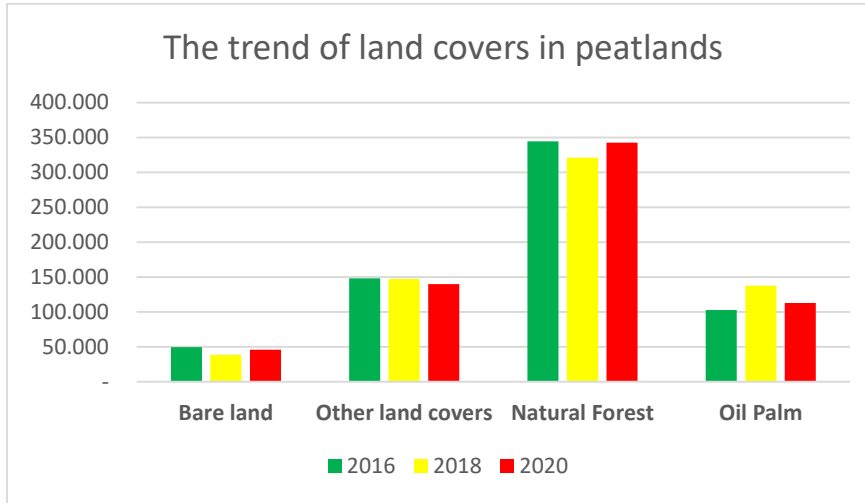
Confusion matrix of PCC 2020

Predicted	Reference						
	Land cover class	bare land	natural forest	other land cover	oil palm	water	Total
bare land	6	1	4	1	0	12	
natural forest	0	69	2	4	0	75	
other land cover	1	1	28	2	0	32	
oil palm	0	4	1	21	1	27	
water	0	0	0	0	4	4	
Total	7	75	35	28	5	150	

5. The trend of land cover types in the study area

The trend was acquired from the best method in this study over time (Post-classification composition)

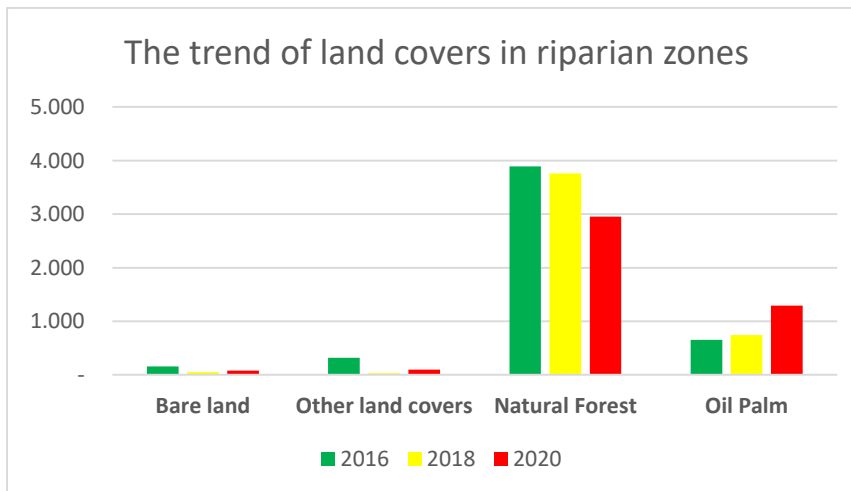
a. Peatlands



The trend of land covers in peatlands

Land cover	Total area (ha)		
	2016	2018	2020
Bare land	49,690	38,634	45,719
Other land covers	148,392	147,385	139,987
Natural Forest	344,675	321,314	342,846
Oil Palm	102,858	137,495	112,863

b. Riparian zones



The trend of land covers in riparian zones

Land cover	Total area (ha)		
	2016	2018	2020
Bare land	160	53	79
Other land covers	320	33	100
Natural Forest	3,891	3,760	2,955
Oil Palm	655	744	1,290

6. Coding

The coding is inspired from <https://github.com/rvmaretto/deepgeo> by Raian Vargas Maretto

a. Generating Train and Test data

#Import Necessary Libraries

```
import numpy as np
import gdal
import skimage
import deepgeo.common.geofunctions as gf
import deepgeo.common.visualization as vis
import deepgeo.dataset.dataset_generator as dg
import deepgeo.dataset.preprocessor as prep
import deepgeo.dataset.sequential_chips as seqchips
import deepgeo.networks.model_builder as mb
from deepgeo.dataset import rasterizer
```

#Defining Input Files

```
local_dir = 'path to your folder'
raster_file = 'path to your tif file'
shape_file = 'path to your shape file'
```

#Visualizing Raster Image

```
img_raster = gf.load_image(TIF file, no_data = 0)
vis.plot_rgb_img(TIF file, bands=[0, 5, 2 ], contrast=True, title="Satellite imagery ")
```

#Rasterizing Shape File

```
classes_of_interest = ['list of your land covers assigned']
non_class = 'a land cover class assigned'
class_column = 'column in the attribute'
out_labels = 'path to your output tif file'
```

```
rstzr = rasterizer.Rasterizer(shape_file,
                             raster_file,
```

```
        class_column,
        classes_interest=classes_of_interest,
        non_class_name=non_class)

rstzr.collect_class_names()
rstzr.rasterize_layer()
class_names = ['no_data'] + rstzr.get_class_names()
rasterized_layer = rstzr.get_labeled_raster()

vis.plot_labels(rasterized_layer,class_names, colors=['white','pink', 'red', 'green', 'black',
'orange', 'blue'],title = 'rasterized full area')

rstzr.save_labeled_raster_to_gtiff(out_labels)
```

#Preprocessing the dataset

```
output_ds = 'path to your dataset'
ds_file_name = 'name of your dataset'

dataset_description = {'years': 2020,
                      'standardization': 'norm_range',
                      'indexes_to_compute': 'none',
                      'bands': ['bands'],
                      'sensor': 'Satellites',
                      'classes':class_names,
                      'img_no_data': 0,
                      'chip_size': 300,
                      'tolerance_nodata': 0.2,
                      'notes': }

preproc = prep.Preprocessor(raster_file, no_data = 0)
```

#Generating Chips

```
generator = dg.DatasetGenerator([raster_img],
                                [rasterized_layer],
                                #strategy='random',
                                strategy='sequential',
                                description=dataset_description)
params = {'win_size': dataset_description['chip_size'],
          'class_of_interest': classes_of_interest,
          'class_names':class_names}
generator.generate_chips(params)
chip_struct = generator.get_samples()
vis.plot_chips(chip_struct, raster_img, bands=[0, 5, 1], contrast=True)
generator.remove_no_data(tolerance=dataset_description['tolerance_nodata'])
```

#Splitting the dataset 80% training and 20% test

```
generator.shuffle_ds()
generator.split_ds(perc_test=20, perc_val=0)
```



```
chip_struct = generator.get_samples()
generator.save_to_disk(output_ds, ds_file_name)
```

b. Training

#Import Necessary Libraries

```
import numpy as np
import gdal
import os
import deepgeo
import deepgeo.networks.model_builder as mb
import deepgeo.networks.loss_functions as lossf
```

#Defining the files

```
model_dir = 'name of your model'
train_tfrecord = 'path to train dataset'
test_tfrecord = 'path to test dataset'
```

#Calculating the weights over land cover classes

```
weights_train = lossf.compute_weights_mean_proportion(train_tfrecord, ['list of land
covers assigned'], classes_zero=['no_data'])
weights_eval = lossf.compute_weights_mean_proportion(test_tfrecord, ['list of land
covers assigned'], classes_zero=['no_data'])
```

#Hyperparameter setting

```
params = {
    'network': 'unet',
    'epochs': number of epochs,
    'batch_size': number of batch_size,
    'chip_size': size of the chip',
    'bands': number of bands,
    'learning_rate': number of learning rate,
    'learning_rate_decay': True,
    'decay_rate': number of decay rate,
    'l2_reg_rate': 0.0005,
    'chips_tensorboard': 2,
    'loss_func': 'weighted_cross_entropy',
    'data_aug_ops': ['rot90', 'rot180', 'rot270', 'flip_left_right',
                    'flip_up_down', 'flip_transpose'],
    'data_aug_per_chip': 6,
    'class_weights': {'train': weights_train, 'eval': weights_eval},
    'num_classes': 7,
    'class_names': ['list of land covers assigned']
    'num_compositions': 1,
    'bands_plot': [1, 5, 2],
    'Notes': 'satellite'
```

#Model training

```
model = mb.ModelBuilder(params)
model.train(train_tfrecord, test_tfrecord, model_dir)
```

c. Prediction

#Import Necessary Libraries

```
import numpy as np
import gdal
import os
import deepgeo.common.geofunctions as gf
import deepgeo.common.visualization as vis
import deepgeo.dataset.dataset_generator as dg
import deepgeo.dataset.preprocessor as prep
import deepgeo.dataset.sequential_chips as seqchips
import deepgeo.networks.model_builder as mb
```

#Pre-processing The Predicted Image

```
raster_file = 'path to the satellite image that want to be predicted'
preproc = prep.Preprocessor(raster_file, no_data = 0)
raster_array = preproc.get_array_stacked_raster()
```

#Generating Chips over The Predicted Image

```
params_cg = {'raster_array': raster_array,
             'overlap': [184,184],
             'win_size': 300}
```

```
chip_struct = seqchips.SequentialChipGenerator(params_cg).generate_chips()
```

#Prediction

```
trained_model = 'path to your trained model'
model = mb.ModelBuilder(trained_model)
chips = model.predict(chip_struct, model_dir=trained_model)
```

```
output_pred = 'path to the predicted file image in tif format'
preproc = None
raster_array = None
gf.write_pred_chips(output_pred, raster_file, chips, chip_key='predict')
pred_rarr = gdal.Open(output_pred).ReadAsArray()
```

#Visualization of the predicted image

```
vis.plot_labels(pred_rarr, ['list of land covers assigned'], colors = ['list of colors'],title= title
of the predicted image')
```

